

1 **Estimating irrigation water use from remotely sensed evapotranspiration**
2 **data: Accuracy and uncertainties at field, water right, and regional scales**

3
4 **Authors:** Sam Zipper^{1,2,*}, Jude Kastens³, Timothy Foster⁴, Brownie Wilson¹, Forrest Melton⁵,
5 Ashley Grinstead^{1,6}, Jillian M. Deines⁷, James J. Butler¹, Landon T. Marston⁸

6
7 **Affiliations:**

- 8 1. Kansas Geological Survey, University of Kansas, Lawrence KS 66047
- 9 2. Department of Geology, University of Kansas, Lawrence KS 66045
- 10 3. Kansas Biological Survey & Center for Ecological Research, University of Kansas,
11 Lawrence KS 66047
- 12 4. School of Engineering, University of Manchester, Manchester, UK
- 13 5. Atmospheric Science Branch, Earth Science Division, NASA Ames Research Center,
14 Moffett Field, CA 94035
- 15 6. Department of Natural Resources and the Environment, University of Connecticut,
16 Storrs, CT 06269, United States
- 17 7. Earth Systems Predictability and Resiliency Group, Pacific Northwest National
18 Laboratory, Richland, WA 99354
- 19 8. Department of Civil and Environmental Engineering, Virginia Tech, Blacksburg VA
20 24061

21 *Correspondence to samzipper@ku.edu

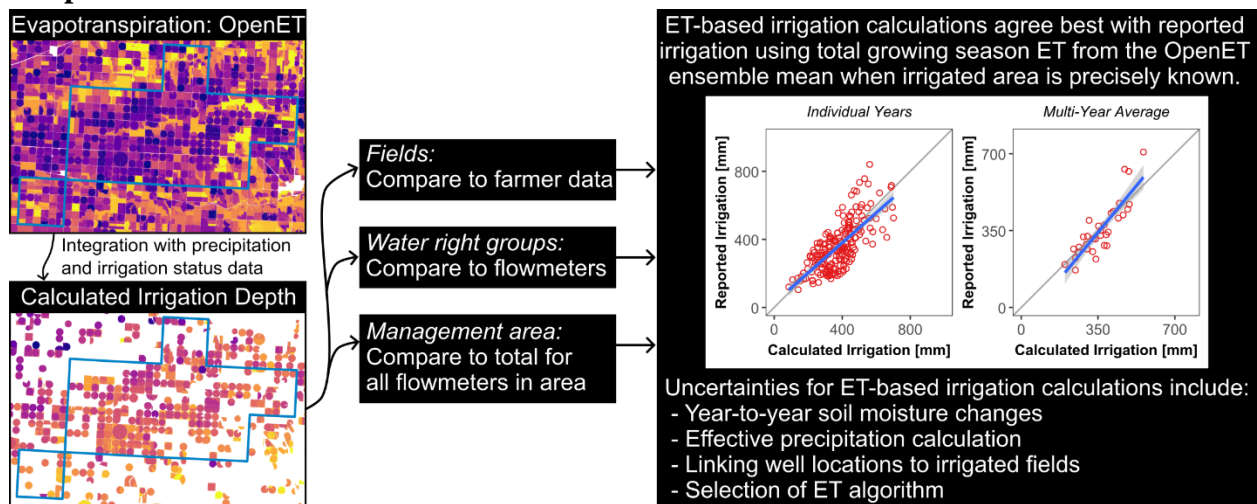
22
23 *This is a revised manuscript submitted to Agricultural Water Management for peer review*
24 *(July 17, 2024).*
25

26 **Abstract**

27 Irrigated agriculture is the dominant user of water globally, but most water withdrawals are not
28 monitored or reported. As a result, it is largely unknown when, where, and how much water is
29 used for irrigation. Here, we evaluated the ability of remotely sensed evapotranspiration (ET)
30 data, integrated with other datasets, to calculate irrigation water withdrawals and applications in
31 an intensively irrigated portion of the United States. We compared irrigation calculations based
32 on an ensemble of satellite-driven ET models from OpenET with reported groundwater
33 withdrawals from hundreds of farmer irrigation application records and a statewide flowmeter
34 database at three spatial scales (field, water right group, and management area). At the field
35 scale, we found that ET-based calculations of irrigation agreed best with reported irrigation when
36 the OpenET ensemble mean was aggregated to the growing season timescale (bias = 1.6% to
37 4.9%, $R^2 = 0.53$ to 0.74), and agreement between calculated and reported irrigation was better for
38 multi-year averages than for individual years. At the water right group scale, linking pumping
39 wells to specific irrigated fields was the primary source of uncertainty. At the management area
40 scale, calculated irrigation exhibited similar temporal patterns as flowmeter data but tended to be
41 positively biased with more interannual variability. Disagreement between calculated and
42 reported irrigation was strongly correlated with annual precipitation, and calculated and reported
43 irrigation agreed more closely after statistically adjusting for annual precipitation. The selection
44 of an ET model was also an important consideration, as variability across ET models was larger
45 than the potential impacts of conservation measures employed in the region. From these results,
46 we suggest key practices for working with ET-based irrigation data that include accurately
47 accounting for changes in soil moisture, deep percolation, and runoff; careful verification of
48 irrigated area and well-field linkages; and conducting application-specific evaluations of
49 uncertainty.

50

51 **Graphical Abstract**



52

53

54 **Keywords:** OpenET, remote sensing, evapotranspiration, water management, High Plains
55 Aquifer, uncertainty

56 **1. Introduction**

57 Irrigated agriculture is the dominant global user of water. Groundwater supplies an
58 estimated 40% of global irrigation, with this figure rising even higher in semi-arid/arid regions or
59 in drought years when surface water availability is limited (Gleeson et al., 2020). As such,
60 groundwater use plays a critical role in global food production and trade (Dalin et al., 2017) and
61 sustaining local and regional economies (Deines et al., 2020). However, groundwater use can
62 also lead to detrimental outcomes, such as the depletion of interconnected surface water
63 resources (de Graaf et al., 2019; Zipper et al., 2022), declining water levels and storage capacity
64 in regionally and globally important aquifers (Hasan et al., 2023; Jasechko et al., 2024), and
65 associated water scarcity and insecurity (D’Odorico et al., 2019; Marston et al., 2020). In many
66 agricultural settings without alternative water sources, pumping reductions are the only currently
67 viable tool available to reduce water abstraction and water table decline rates (Butler et al.,
68 2020).

69 Making informed management decisions requires information about pumping rates and
70 the anticipated impacts on the environment (Foster et al., 2020). However, management is
71 challenging because data on the locations, schedules, and volumes of groundwater withdrawals
72 are rarely available, even in data-rich countries like the United States (Marston, Abdallah, et al.,
73 2022). Given the paucity of groundwater pumping data, emerging application-ready remote
74 sensing products may be a valuable tool to fill this data gap (Melton et al., 2022). While
75 flowmeters on pumping wells directly monitor the amount of water coming out of the ground,
76 which we refer to here as ‘irrigation water withdrawals’, remotely sensed approaches typically
77 provide data for spatially distributed evapotranspiration (ET) rates. Satellite-based ET data can
78 then be incorporated into a water balance or statistical model to infer ‘irrigation water
79 applications’, or the amount of water that is applied to a field after accounting for losses
80 (Dhungel et al., 2020; Folhes et al., 2009; Foster et al., 2019; Laluet et al., 2024). These models
81 can range from simple annual water balances to detailed daily soil water balance models tracking
82 multiple components of the water balance such as infiltration, deep percolation, and runoff. Like
83 all modeled quantities, however, these ET-based calculations of irrigation are subject to
84 numerous uncertainties, which can lead to inefficient or inequitable water management decisions
85 if not well-characterized (Foster et al., 2020).

86 Unfortunately, due to the lack of reliable irrigation water withdrawal and application data
87 for ground reference, there have been limited opportunities to evaluate the ability of ET-based
88 approaches to calculate irrigation withdrawals and applications. While many past studies have
89 sought to estimate irrigation water use using satellite-based ET data and other hydrological
90 variables such as soil moisture (Brocca et al., 2018; Dari et al., 2020; Ketchum et al., 2023),
91 these estimates have typically been evaluated against aggregated statistics or synthetic model
92 estimates of water use. Other studies use statistical or machine learning approaches to relate ET
93 to observed water use, but these approaches are limited in terms of their applicability outside of
94 the model training region (Filippelli et al., 2022; Majumdar et al., 2022; Wei et al., 2022). As a
95 result, there is a lack of knowledge about how effectively ET data can be translated into

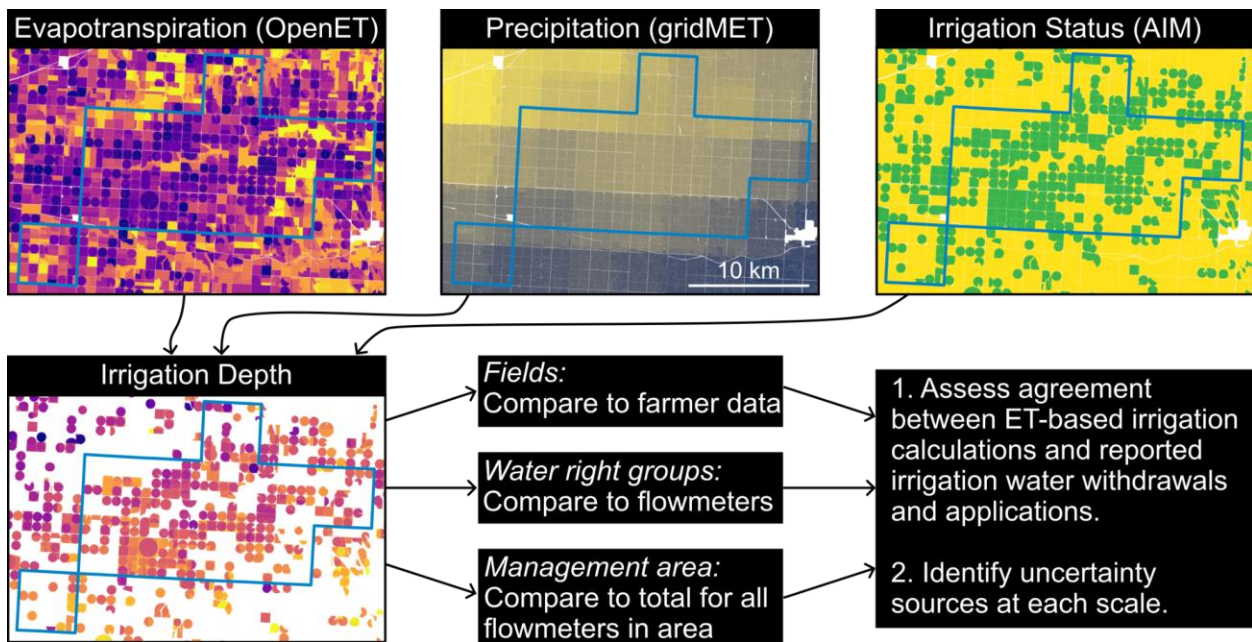
96 irrigation water withdrawals and applications across different spatial scales, from an individual
 97 field to a region, which are relevant to regulatory and management purposes.

98 Here, we address this gap by comparing calculations of ET-based irrigation applications
 99 and reported irrigation at multiple spatial scales (field, water right group, management area)
 100 within the heavily irrigated High Plains Aquifer in the State of Kansas (USA). Reported
 101 irrigation data are from both direct farmer-provided records of irrigation water applications and a
 102 high-quality flowmeter database of irrigation water withdrawals (Figure 1). Specifically, we ask:

- 103 (1) How well do irrigation calculations derived from remotely sensed data and other spatial
 104 datasets agree with water withdrawal and application data from flowmeters and farmer
 105 records?
 106 (2) What are the major sources of uncertainty in calculating irrigation withdrawals and
 107 applications using remotely sensed ET data?

108 Addressing these questions provides insights into the potential for remotely sensed ET products
 109 to address critical water challenges and highlights key future research needed to operationalize
 110 ET data for agricultural water management.

111



112

113 **Figure 1.** Overview of study including key input datasets (OpenET: Melton et al., 2022; gridMET:
 114 Abatzoglou, 2013; AIM: Deines, Kendall, Crowley, et al., 2019), spatial scales, and study objectives. The
 115 images show the area in and around the Sheridan-6 Local Enhanced Management Area (blue outline), the
 116 location of which is shown in Figure 2.

117

118 **2. Methods**

119

120 *2.1 Study areas and irrigation ground data*

121 We conducted comparisons of ET-based irrigation calculations to in-situ measurements of
122 groundwater withdrawals and applications at three spatial scales that address different potential
123 use cases for remotely sensed irrigation data:

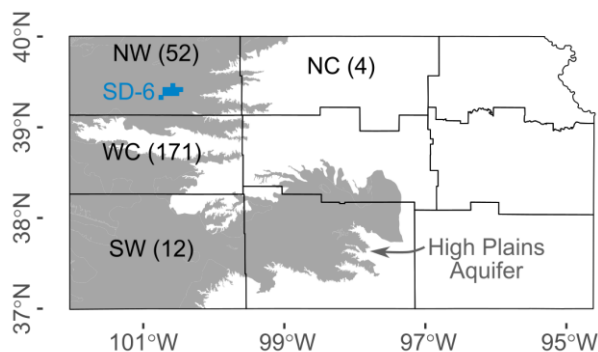
124 (1) At the field scale (Section 2.1.1), we compared ET-based calculated irrigation depths to
125 field-resolution irrigation water application data from fields where farmers voluntarily
126 shared irrigation records (field-years of data by region shown in Figure 2 in parenthesis).

127 (2) At the water right scale (Section 2.1.2), we focused on a 255 km² groundwater
128 management area, the Sheridan-6 Local Enhanced Management Area (SD-6 LEMA; blue
129 area in Figure 1 and Figure 2). We subdivided the SD-6 LEMA into water right groups
130 (WRGs) made up of non-overlapping combinations of pumping wells, fields, and
131 authorized places of use and compared ET-based irrigation volumes to total water
132 withdrawals within each WRG.

133 (3) At the management area scale (Section 2.1.2), we compared ET-based irrigation volumes
134 to total reported irrigation water withdrawals within the entire SD-6 LEMA.

135 Conducting our analysis at these three spatial scales allowed us to leverage independent data
136 sources for comparison (farmer records at the field scale, a state database at the water right and
137 management area scales) and assess different aspects of uncertainty.

138



139

140 **Figure 2.** Map of the state of Kansas subdivided into agricultural reporting districts. The number of field-
141 years of data at the field scale are shown in parentheses for the northwest (NW), north-central (NC), west-
142 central (WC), and southwest (SW) reporting districts within the state. The location of the Sheridan-6 (SD-
143 6) Local Enhanced Management Area is shown in blue. The Kansas portion of the High Plains Aquifer is
144 shown in gray.

145

146 2.1.1 Individual fields

147 We collected field-resolution irrigation application information from four farmers willing
148 to share this information with us. Farmers were contacted directly based on existing personal
149 relationships and through regional organizations such as groundwater management districts and
150 asked to provide applied irrigation volumes for as many fields as they were willing to share at

151 the finest possible temporal resolution. We also requested either data files or annotated pictures
152 showing the irrigated extent for each field so we could extract satellite-based ET data for each
153 field. Therefore, unlike the management area and WRG scale comparisons described in Section
154 2.1.2, for the field-scale comparison we had information on actual places of use and irrigated
155 extent. Irrigation data varied in format, including minute-resolution water use from irrigation
156 control software, irregularly timed sub-annual water use based on periodic visits to flowmeters,
157 and annual values based on flowmeter data that farmers associated with specific fields. For this
158 study, all data were aggregated to the annual total depth of applied irrigation. In total, we
159 received data for 43 fields between 2016 and 2022, totaling 239 field-years of data. Following
160 Ott et al. (2024), we screened out any fields where the ratio of irrigation to the difference of ET
161 (from the OpenET ensemble mean) and effective precipitation was <0.5 or >1.5 , since this
162 suggests potential errors in reported irrigation data. To protect the privacy of the farmers
163 involved (Zipper, Stack Whitney, et al., 2019), the locations of the fields are only shown here at
164 the resolution of federal agricultural reporting districts (Figure 2). The data span three of the five
165 reporting districts that overlie the High Plains Aquifer, with the most fields in west-central and
166 northwest Kansas (note: one field, just across the border in Nebraska, is included with the NW
167 Kansas district). None of the fields included within this dataset are within the SD-6 LEMA.

168

169 2.1.2 Sheridan-6 Local Enhanced Management Area

170 The SD-6 LEMA covers 255 km² in northwest Kansas, much of which is used to grow
171 irrigated corn, soybeans, sorghum, and wheat (Figure 2). The SD-6 LEMA was formed when
172 local irrigators, concerned about declining groundwater levels, proposed an allocation of 1397
173 mm (55”) of water over a five-year period, which represented an approximate 20% reduction in
174 pumping rates compared to historical averages (Drysdale & Hendricks, 2018). After approval by
175 the state’s chief engineer, this allocation was codified in law for a five-year period beginning in
176 2013. The irrigators within the SD-6 LEMA have since renewed for two additional five-year
177 periods (2018-2022 and 2023-2027). To date, the SD-6 LEMA exceeded the original
178 conservation goals and reduced irrigation water withdrawals by 26-31% (Deines, Kendall,
179 Butler, et al., 2019; Drysdale & Hendricks, 2018) and slowed water table decline rates (Butler et
180 al., 2020; Whittemore et al., 2023) with only minor negative impacts on yield and none on
181 profitability (Golden, 2018). As such, the SD-6 LEMA is a successful example of irrigator-
182 driven groundwater conservation (Marston, Zipper, et al., 2022) and has motivated the
183 development of additional conservation approaches around the state (Steiner et al., 2021).

184 We selected the SD-6 LEMA as the focus of our management area and water right scale
185 comparison because conservation practices have led to high irrigation efficiencies of producers
186 in the SD-6 LEMA with relatively little wasted irrigation water (e.g., deep percolation from
187 return flows or major fluxes of soil evaporation caused by excessive irrigation; Deines et al.,
188 2021). High irrigation efficiency suggests that irrigation water withdrawals and applications
189 should be approximately equal, and ET-based approaches should be particularly effective for
190 calculating irrigation volumes in this setting. Additionally, due to numerous past studies of

191 groundwater use in the SD-6 LEMA (Deines et al., 2021; Deines, Kendall, Butler, et al., 2019;
192 Dhungel et al., 2020; Drysdale & Hendricks, 2018; Glose et al., 2022; Whitemore et al., 2023),
193 we have a high degree of confidence in the accuracy of the irrigation withdrawal data for the SD-
194 6 LEMA.

195 Irrigation withdrawal data were aggregated from the Water Information Management and
196 Analysis System (WIMAS; <https://geohydro.kgs.ku.edu/geohydro/wimas/>) database maintained
197 by the Kansas Department of Agriculture - Division of Water Resources and the Kansas
198 Geological Survey. Withdrawal data are at the resolution of points of diversion, which in the SD-
199 6 region correspond exclusively to pumping wells since there are no surface water resources used
200 for irrigation. The data are high quality, as all non-domestic pumping wells in the state of Kansas
201 are required to use a totalizing flow meter subject to accuracy checks from the Kansas
202 Department of Agriculture with strong penalties for falsifying flow meter data or drilling illegal
203 wells (Butler et al., 2016). Therefore, we do not believe there is significant under-reported or
204 non-reported irrigation water use in the area. The WIMAS database also includes reported total
205 irrigated acreage in each year, though unlike water use, the reported irrigated acreage is not
206 subject to verification and therefore the accuracy is unknown. In the SD-6 LEMA, we conducted
207 our comparison at two spatial scales:

- 208 ● For the water right group (WRG) scale comparison, we established non-overlapping
209 groups of water withdrawals and applications by combining wells, water rights, and
210 authorized places of use as in Earnhart & Hendricks (2023). This aggregation was
211 necessary due to the complexities of agricultural water management that make it
212 impossible to quantify the water use for a specific field from the WIMAS data alone: (i) a
213 single well may provide water to multiple fields; (ii) a single field may receive water
214 from multiple wells; (iii) a single water right may cover multiple wells and fields; and
215 (iv) irrigators are only required to report the authorized place of use and the total number
216 of acres irrigated, not the specific locations where water was used within the authorized
217 area in a specific year. For each WRG, we then summed the total reported annual water
218 withdrawals for all wells within the WRG.
- 219 ● For the management area scale comparison, we summed the total annual withdrawals
220 from all irrigation wells within the SD-6 LEMA boundaries. For any water rights that had
221 authorized places of use both inside and outside the LEMA ($n = 9$, or 6% of the total
222 water right groups), we scaled the total water use based on the proportion of total
223 estimated irrigated area that was within the LEMA for that well. This is the approach
224 used in Brookfield et al. (2023) and is extended here through additional analyses of
225 uncertainty, the use of effective precipitation for estimating irrigation depths, and
226 comparison to other spatial scales.

227 The SD-6 LEMA comparisons were conducted for the period 2016-2020, as that is the extent
228 covered by all necessary input datasets (described in Section 2.2).

229

230 *2.2 Calculating irrigation from ET data*

231 We integrated ET data with several other geospatial datasets to calculate irrigation
232 volumes and/or depths (Figure 1). We extracted OpenET data from Google Earth Engine at a
233 monthly time step for 2016-2022 (Melton et al., 2022). OpenET includes ET data from six
234 different satellite-driven models, as well as an ensemble mean. The models included are
235 DisALEXI (Anderson et al., 2007, 2018), eeMETRIC (Allen et al., 2005, 2007, 2011),
236 geeSEBAL (Bastiaanssen et al., 1998; Laipelt et al., 2021), PT-JPL (Fisher et al., 2008), SIMS
237 (Melton et al., 2012; Pereira, Paredes, Melton, et al., 2020), and SSEBop (Senay et al., 2022).
238 The ensemble mean was calculated as the mean of all models, with outlier values from the
239 ensemble identified based on median absolute deviations and removed prior to averaging (Volk
240 et al., 2024). The OpenET products were validated against 70 eddy covariance towers deployed
241 at agricultural sites spanning a range of climate and land cover conditions across the western US
242 and generally had a strong agreement, with all models within +/- 15% of growing season mean
243 flux tower ET averaged across all sites (Melton et al., 2022). A subsequent evaluation affirmed
244 the accuracy of the ET data from OpenET via comparison to a total of 141 sites with eddy
245 covariance towers, along with seven sites with Bowen ratio systems and four weighing
246 lysimeters, finding that the growing season ensemble ET values for cropland had a mean
247 absolute error of 78.1 mm (13.0%) and a mean bias error of -11.9 mm (2.0%). The overall
248 accuracy for cropland sites was the best of any land cover type evaluated, and performance for
249 annual crops, including corn, soybeans, and wheat, was particularly strong (Volk et al., 2024).
250 However, there were no eddy covariance towers near our study area - the closest irrigated fields
251 with eddy covariance towers were in Mead, NE, where annual precipitation is ~50% greater than
252 western Kansas - and therefore OpenET's accuracy for irrigated agriculture in semi-arid
253 conditions typical of the western High Plains Aquifer has not been locally assessed.

254 OpenET data and precipitation data (from the 4 km gridMET data; Abatzoglou, 2013)
255 were averaged for each field. For the field-resolution comparison, field boundaries, crop type,
256 and irrigation status were defined based on information provided by farmers. For the
257 management area and WRG comparisons, field boundaries were defined based on a Kansas-
258 specific modification of the US Department of Agriculture (USDA) Common Land Unit dataset
259 (Gao et al., 2017; MardanDoost et al., 2019), annual crop type from the USDA Cropland Data
260 Layer (USDA, 2022), and field-resolution irrigation status from the Annual Irrigation Maps
261 (AIM) dataset (Deines, Kendall, Crowley, et al., 2019). For crop type and irrigation status, we
262 summarized the rasterized input data to a single categorical value for each field based on the
263 most common raster value.

264 To estimate irrigation using our ET data (Figure 1), we calculated the precipitation deficit
265 (ET - effective precipitation) for each field (Figure S1) and masked it to only fields mapped as
266 irrigated by AIM (Figure S2). Effective precipitation was calculated as precipitation from
267 gridMET minus deep percolation out of the bottom of the root zone, which we estimated as a
268 function of precipitation based on 2013-2017 deep percolation estimates from Deines et al.
269 (2021) (regressions shown in Figure S3). This method does not account for soil moisture storage

270 from year-to-year, so we did these calculations at three timescales: the growing season (April-
271 October), the calendar year (January-December), and the water year (October-September). This
272 allowed us to test the degree to which the timescale of aggregation influenced agreement
273 between calculated and reported irrigation withdrawal data. Since negative irrigation depths are
274 not physically possible, for any irrigated fields with a negative precipitation deficit we set the
275 irrigation depth to 0 mm, though this was rare and negative precipitation deficits were typically
276 associated with fallow, non-irrigated fields (Figure S1). Irrigation depth was calculated
277 separately for each year and each model (six ET models, as well as the ensemble mean). To
278 convert field-resolution irrigation depths to irrigation volumes for comparison with pumping
279 data, we multiplied the calculated irrigation depth by the area within each field that was mapped
280 as irrigated in AIM. Since there are no surface water rights in this region, we assumed that all
281 irrigation was sourced from groundwater.

282

283 *2.3 Assessing approaches for improving irrigation calculations*

284 Our approach to estimating irrigation adopts several assumptions, including that there is
285 minimal runoff or fluxes of water apart from precipitation, irrigation, deep percolation and
286 evaporation. While past work has suggested that there is virtually no runoff under conservation
287 practices in the SD-6 LEMA (Deines et al., 2021), these assumptions may be less appropriate in
288 other parts of the state, in particular the 4 field-years of data in the north-central region (Figure
289 2). Additionally, there may be differences in the relationship between precipitation and deep
290 percolation in other regions given that irrigation efficiency is particularly high in the SD-6
291 LEMA.

292 We assessed both our confidence in and potential impacts of errors in irrigated area
293 classification. In the SD-6 LEMA area, we evaluated confidence in the field-resolution irrigation
294 classifications by evaluating the area of fields with a mixture of irrigated and non-irrigated pixels
295 in the AIM dataset. The irrigation confidence results suggested that this irrigation status mapping
296 approach was more likely to overestimate, rather than underestimate, irrigated area (Figure S4,
297 Figure S5) due to field boundaries not perfectly aligning with on-the-ground management
298 divisions. To address this, we used the fraction of each field that was mapped as irrigated to scale
299 from calculated irrigation depths to irrigation volumes so that potentially non-irrigated portions
300 of otherwise irrigated fields were not included in volume estimation. To determine the potential
301 impacts of uncertainty in irrigated area on our results, as well as potential errors associated with
302 defining WRGs, we also compared reported irrigated acreage for all the wells in the WRG (from
303 the WIMAS database) to the estimated irrigated acreage from AIM for irrigated fields in the
304 WRG. We then repeated our comparison of WRG-scale reported and calculated irrigation water
305 use for only WRGs where the reported and estimated irrigated area agreed within 10%.

306 Additionally, at the management area scale, we evaluated the degree to which a locally-
307 informed bias correction approach could be used to improve agreements between calculated and
308 reported irrigation. This approach, which we call ‘precipitation-adjusted irrigation calculations’,
309 involved developing a linear regression between the irrigation volume residual and precipitation,

310 and then using this linear relationship to adjust ET-based irrigation calculations. This adjustment
311 is useful in both highlighting potential mechanisms for disagreement between calculated and
312 observed irrigation and to demonstrate an approach for either spatial or temporal extrapolation
313 from locations/time periods with well-monitored irrigation to locations/time periods where
314 irrigation is not monitored.

315

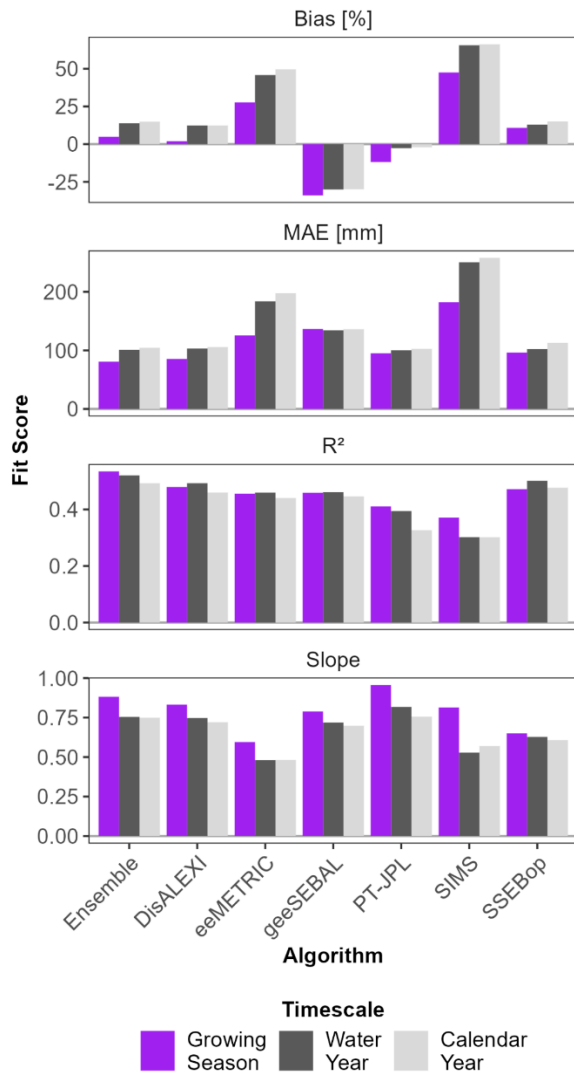
316 **3. Results**

317 *3.1 Field-scale comparison*

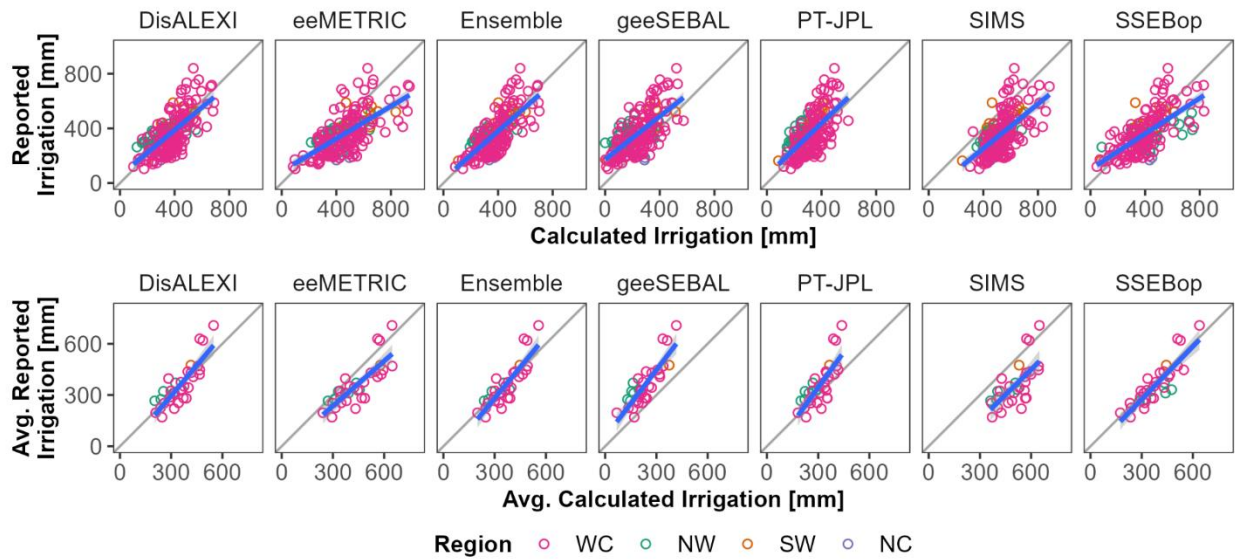
318 At the field scale, we first evaluated the timescale for aggregating the calculated
319 precipitation deficit at which calculated and reported irrigation agreed best. We found that using
320 the growing season for aggregation consistently provided the best agreement in terms of percent
321 bias, mean absolute error (MAE), slope of the relationship between calculated and reported
322 irrigation, and R^2 (Figure 3). This was true across most ET algorithms and fit metrics, and for all
323 subsequent analyses at the field, WRG, and management area scale, we used the growing season
324 timescale of aggregation for irrigation calculations. Slope values tended to be <1 for all ET
325 models at the annual scale (Figure 3, Table 1). The slope of the relationship between calculated
326 and reported irrigation can be an indicator of irrigation efficiency (Ott et al., 2024), and the slope
327 < 1 may reflect lower irrigation efficiencies and increased non-evaporative losses (such as deep
328 percolation or runoff), particularly since our effective precipitation relationship was based on the
329 data from the SD-6 LEMA and the field-scale analysis did not include fields within the LEMA
330 (Figure S3). Agreement for individual years did not appear to vary systematically as a function
331 of the region within the state, though the dataset was not evenly distributed among regions with
332 most of the fields in either west-central or northwest Kansas (71.5% and 21.8% of total field-
333 years, respectively; Figure 2) which are climatically very similar.

334 Comparing across OpenET models, we found that the OpenET ensemble mean tended to
335 provide the best agreement with reported irrigation at the annual timescale, with a MAE of 81
336 mm, bias of 4.9%, slope of 0.88, and R^2 of 0.53 (Table 1). This slope (0.88) closely matches
337 typical irrigation efficiencies for the region (0.9; Deines et al., 2021), suggesting that losses in
338 the irrigation conveyance system and wind-drift evaporation are approximately 12% of pumped
339 water. When averaged across multiple years, the error in each model was substantially reduced
340 (Figure 4, Table 1). The choice of model also contributed to variability for both individual years
341 and multi-year averages. While the ensemble mean provided the best overall agreement between
342 calculated and reported data, there was also good agreement with reported data for irrigation
343 calculations using DisALEXI and PT-JPL. In contrast, eeMETRIC and SSEBop tended to
344 overestimate at high levels of irrigation, geeSEBAL tended to underestimate across the range of
345 irrigation depths, and SIMS tended to overestimate across the range of irrigation depths (Figure
346 4). The high calculated irrigation volumes from SIMS make sense due to the formulation of this
347 model, which assumes well-watered conditions sufficient to meet the needs of the satellite-
348 observed crop density (Melton et al., 2012). Even irrigated crops in this region likely experience

349 periodic water stress during the growing season, as evidenced by the narrow distribution of
 350 SIMS ET data with respect to other models (Figure S6).
 351



352
 353 **Figure 3.** Agreement between field-resolution reported and calculated irrigation based on different
 354 aggregation timescales. Fit metrics shown include bias (better performance = closer to 0), mean absolute
 355 error (MAE; better performance = closer to 0), R² (better performance = closer to 1), and slope (better
 356 performance = closer to 1).



358

359 **Figure 4.** Comparison between reported and calculated irrigation for individual fields. The top row shows
 360 annual irrigation and the bottom row shows the multi-year average, both colored by the region within the
 361 state. Calculated irrigation is based on growing season timescale of aggregation. In each panel, the gray
 362 line indicates 1:1 agreement and the blue lines in the bottom panels show a linear best-fit with a shaded
 363 standard error confidence interval.

364

365 **Table 1.** Fit statistics for field-resolution comparison between calculated and reported irrigation
 366 application depths based on growing season timescale of aggregation.

Model	MAE [mm]		Bias [%]		Slope		R ²	
	Annual	Multi-Year	Annual	Multi-Year	Annual	Multi-Year	Annual	Multi-Year
DisALEXI	85	52	1.9	-1.5	0.83	1.18	0.48	0.71
eeMETRIC	126	93	27.7	22.7	0.59	0.88	0.46	0.66
Ensemble	81	48	4.9	1.6	0.88	1.22	0.53	0.74
geeSEBAL	136	126	-34.0	-35.2	0.79	1.31	0.46	0.73
PT-JPL	95	69	-11.9	-13.3	0.96	1.38	0.41	0.60
SIMS	182	158	47.5	41.8	0.81	0.99	0.37	0.47
SSEBop	96	52	10.8	6.5	0.65	1.03	0.47	0.76
Average	115	86	6.7	3.2	0.79	1.14	0.45	0.67

367

368 **3.2 SD-6 LEMA water right group comparison**

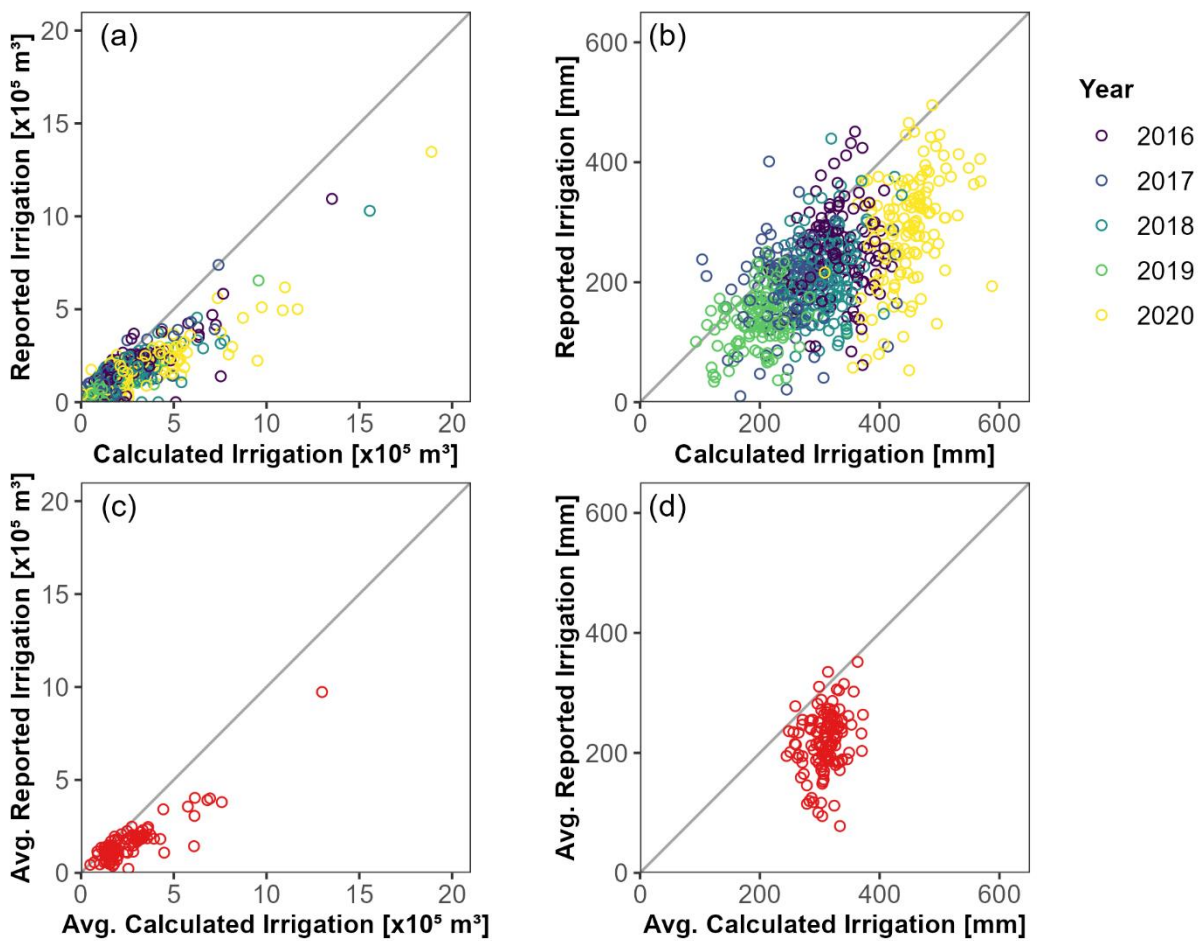
369 For the WRG-scale comparison, the growing season-based irrigation volumes from the
 370 ensemble ET were used, since this had the best agreement at the field scale where there are fewer
 371 sources of uncertainty (Section 3.1). The calculated irrigation volumes showed substantially
 372 more interannual variability than reported irrigation volumes at the WRG scale, with ET-based
 373 irrigation volumes positively biased relative to reported volumes for most WRGs (Table 2).
 374 While there was a positive bias across all years, the greatest positive bias was during dry years

375 such as 2020 (Figure 5a). When averaged across all five years, the scatter in the agreement
376 between estimated and reported irrigation volumes was dramatically reduced (Figure 5c), leading
377 to a decrease in MAE and increase in slope and R^2 relative to the annual-resolution comparison
378 (Table 2).

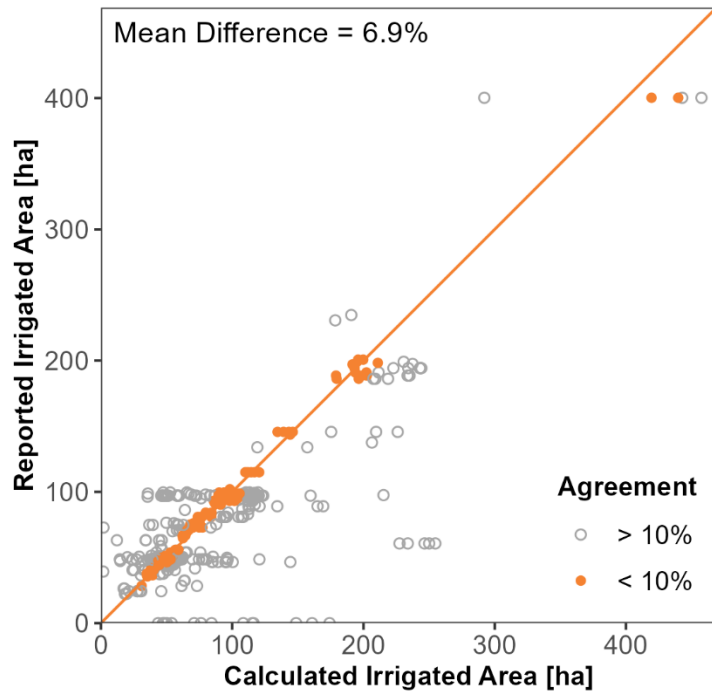
379 The correlation between calculated and reported irrigation was worse for irrigation depths
380 (Figure 5b, Figure 5d) than volumes (Figure 5a, Figure 5c), though irrigation volumes were more
381 consistently positively biased than depths (Table 2). Overall, our results indicate that uncertainty
382 in estimated irrigation depth is greater than uncertainty in estimated irrigated volume, which is
383 further supported by the field-scale comparison in Section 3.1 and has been observed in other
384 ET-based irrigation comparisons in Nevada and Oregon (Ott et al., 2024). Nevertheless, place of
385 use and irrigation status are important potential drivers of disagreement between calculated and
386 reported irrigation volumes. While there was a positive correlation between reported and
387 estimated irrigated area, the irrigated area within WRGs based on AIM only matched the
388 reported irrigated area in the WIMAS database for approximately half of WRG-years (321 of
389 680 within 10%). Differences between reported and calculated irrigated area were mostly
390 distributed around the 1:1 line, with a slight positive bias for calculated irrigated area (Figure 6).
391 On average, the estimated irrigated area was 6.9% higher than the reported irrigated area (median
392 = 1.1%).

393 This disagreement may be due to errors in reported irrigated area and calculated irrigated
394 area as well as difficulties in identifying annual places of use for each WRG. While irrigated area
395 is required for annual water use reports, water use reports do not include spatial information
396 specifying where the water was actually used, and total irrigated area is not subject to
397 verification or enforcement penalties (unlike reported water use). Therefore, it is unknown how
398 accurate the reported data are, but one plausible explanation for the disagreement in estimated
399 and reported irrigated area is uncertainty in field or parcel boundaries, particularly related to
400 corners of parcels that are irrigated with center-pivot systems. Since the field boundary dataset
401 we are using was originally based on 2007 common land units (CLUs) mapped by the USDA
402 with some refinements (Gao et al., 2017), it may not accurately delineate fields that harbor
403 differently managed component areas. For example, a square quarter section containing a center
404 pivot might consist of separate CLUs for the irrigated circle and the non-irrigated corners, or it
405 might simply be the quarter section boundary with multiple records for differently managed
406 subfields used when the farmer signs up for federal government programs such as crop
407 insurance. In the latter case, the entire field would be classified as irrigated based on our
408 assignment of irrigation by majority, even though the ~20% of the field in the corners would not
409 be reported as irrigated by the farmer. This is consistent with our observation that there tended to
410 be more low-confidence classifications for irrigated fields than non-irrigated fields (Figure S4),
411 and supports our approach using the fraction of the field that was mapped as irrigated to scale
412 from calculated irrigation depth to volume (see Section 2.2). Areas of low-confidence
413 classifications were often field corners (Figure S5), suggesting that the misclassification of non-

414 irrigated corners as irrigated due to insufficiently refined field boundaries may have a slight
 415 contribution to overestimated irrigation volumes at both the WRG and management area scales.
 416 To assess the potential impacts of errors in irrigated area classification, we repeated the analysis
 417 using only WRGs and years where the reported and estimated irrigated area agreed within 10%
 418 (Figure 7 and ‘Area Agree’ columns in Table 2). The results of this comparison had a smaller
 419 positive bias for both irrigation volumes and depths, with overall the best agreement observed for
 420 multi-year average volumes (Figure 7c). While the annual-resolution irrigation depths had a
 421 similar overall correlation ($R^2 = 0.35$ in Figure 5b and $R^2 = 0.40$ in Figure 7b), the correlation
 422 between five-year average calculated and reported irrigation depth improved when only using
 423 WRGs with strong irrigated area agreement ($R^2 = 0.32$, Figure 7d) compared to using all WRGs
 424 within the LEMA ($R^2 = 0.05$, Figure 5d).

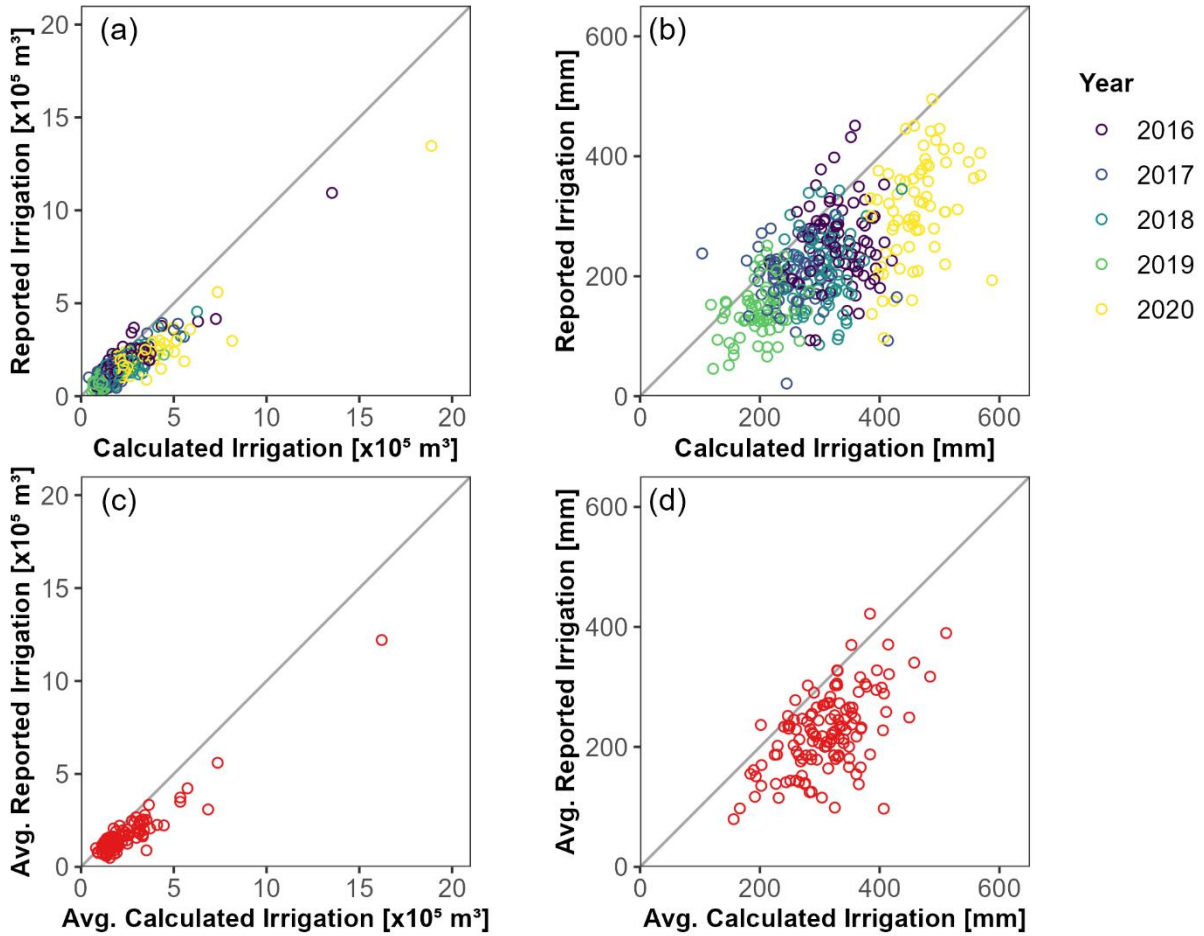


425
 426 **Figure 5.** Comparison of reported irrigation for each water right group (WRG) to ET-based irrigation
 427 calculation using the ensemble ET. (a) Annual irrigation volume for each WRG; (b) Annual irrigation
 428 depth for each WRG; (c) Average irrigation volume for each WRG; (d) Average irrigation depth for each
 429 WRG. In each plot, the gray line shows a 1:1 agreement between reported and estimated irrigation.
 430 Calculated irrigation is based on growing season timescale of aggregation.
 431



432
433
434
435
436

Figure 6. Comparison between reported irrigated area (from WIMAS) and estimated irrigated area (from AIM and authorized places of use) within each water right group in the SD-6 LEMA. Points colored orange have an agreement within 10% and the orange line shows 1:1 agreement.



437
 438 **Figure 7.** Same as Figure 5, but only for WRGs where reported and calculated irrigated area agreed
 439 within 10% (i.e., orange points in Figure 6). Each panel shows: (a) Annual irrigation volume for each
 440 WRG; (b) Annual irrigation depth for each WRG; (c) Average irrigation volume for each WRG; (d)
 441 Average irrigation depth for each WRG. In each plot, the gray line shows a 1:1 agreement between
 442 reported and calculated irrigation. Calculated irrigation is based on growing season timescale of
 443 aggregation.

444
 445 **Table 2.** Fit statistics for WRG comparison for all WRGs (data points shown in Figure 5) and those with
 446 irrigated area agreement (data points shown Figure 7).

Model	MAE		Bias [%]		Slope		R ²	
	All WRGs	Area Agree	All WRGs	Area Agree	All WRGs	Area Agree	All WRGs	Area Agree
Annual Irrigation Volume [x10 ⁵ m ³]	0.92	0.66	57%	40%	0.53	0.64	0.72	0.83
Annual Irrigation Depth [mm]	98.76	93.81	42%	38%	0.54	0.56	0.35	0.40
Average Irrigation Volume [x10 ⁵ m ³]	0.86	0.67	57%	41%	0.57	0.68	0.79	0.89
Average Irrigation Depth [mm]	90.97	89.88	41%	39%	0.44	0.58	0.05	0.32

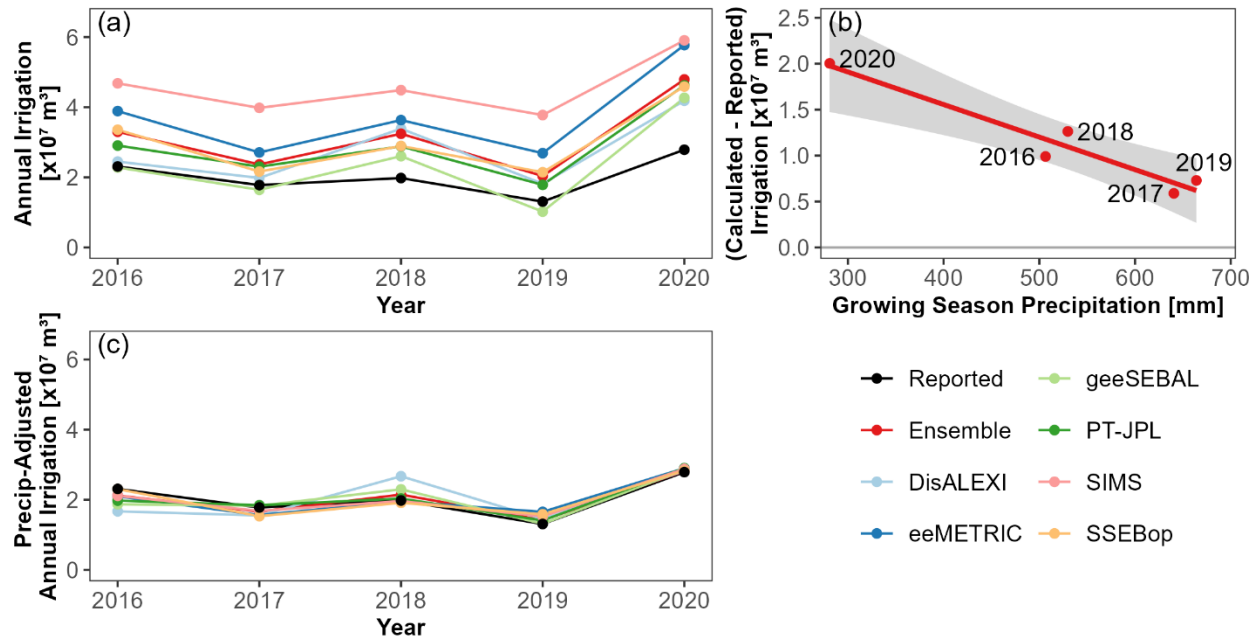
447

448 *3.3 Management area comparison*

449 At the scale of the SD-6 LEMA, the ET-based irrigation volumes are the same order of
450 magnitude as the reported withdrawal volumes but have a positive bias and greater interannual
451 variability (Figure 8a, Table 3). The best-performing model depends on the fit metric being used
452 (Table 3, 'Calc.' column). For instance, the average MAE and bias values were lowest for
453 geeSEBAL, while SIMS had the slope closest to 1 and the ensemble mean and SIMS had the
454 highest R^2 . Since we observed an overestimate across all models, the relatively lower MAE and
455 bias for geeSEBAL reflects its consistently low estimates of ET relative to other algorithms (as
456 observed for the field-scale analysis; Figure 4). The high R^2 values we observe across all models
457 (generally $R^2 \sim 0.9$), combined with the relatively high MAEs ($\sim 0.5\text{-}2.5 \times 10^7 \text{ m}^3$, which is
458 approximately equal to typical irrigation withdrawals for the management area) and a slope
459 substantially lower than one (Table 3) collectively support our interpretation that the ET-based
460 irrigation calculations capture appropriate temporal patterns of variability in estimated irrigation,
461 but tend to overestimate both the average magnitude and degree of interannual variability in
462 irrigation volumes.

463 Subsequent analyses suggest that estimates of non-evaporative components of the water
464 balance, such as deep percolation and root zone soil moisture storage changes, are a potential
465 mechanism for this positive bias and increased variability because they can represent a potential
466 source or sink for water that is not captured by our precipitation deficit calculation. The potential
467 importance of deep percolation and soil moisture storage are suggested by Figure 8b, which
468 shows that growing season precipitation is strongly correlated with the difference between the
469 ET-based irrigation volumes and the reported groundwater withdrawals. The consistent positive
470 bias in all years indicates that our effective precipitation estimates may be too low, while the
471 strong correlation with precipitation suggests that the difference is driven by hydrologic
472 dynamics. The ET-based approaches overestimated the reported irrigation volumes by the
473 greatest amount in dry years, such as 2020, and the smallest amount in wet years, such as 2019
474 (Figure 4a). We found that a precipitation-based bias correction (described in Section 2.3 and
475 shown as precipitation-adjusted annual irrigation in Figure 8c) had a substantially better
476 agreement with reported irrigation values, with reductions in MAE by an order of magnitude,
477 and four of the models and the ensemble mean had slopes between 0.9 and 1.1 after adjustment
478 (Table 3, 'Precip-Adj.' column).

479



480
 481 **Figure 8.** (a) Comparison between reported WIMAS pumping and ET-based irrigation volumes over the
 482 entire SD-6 LEMA. (b) Difference between ET-based calculated irrigation volume (from the OpenET
 483 ensemble) and reported water withdrawals for the SD-6 LEMA as a function of total growing season
 484 precipitation. The red line indicates a linear best-fit with a shaded standard error confidence interval ($R^2 =$
 485 0.93) and points are labeled by year. (c) Comparison of reported and calculated irrigation for the SD-6
 486 LEMA following precipitation adjustment based on Figure 8b. In all panels, calculated irrigation is based
 487 on growing season timescale of aggregation.

488
 489
 490
 491

Table 3. Fit statistics for LEMA-scale OpenET-WIMAS comparison for each timescale of aggregation and model. ‘Calc.’ = calculated irrigation without adjustment (Figure 8a), ‘Precip.-Adj.’ = precipitation-adjusted irrigation (Figure 8c). Calculated irrigation is based on growing season timescale of aggregation.

Model	MAE [$\times 10^7$ m³]		Bias [%]		Slope		R²	
	<i>Calc.</i>	<i>Precip-Adj.</i>	<i>Calc.</i>	<i>Precip-Adj.</i>	<i>Calc.</i>	<i>Precip-Adj.</i>	<i>Calc.</i>	<i>Precip-Adj.</i>
DisALEXI	0.73	0.35	36%	0%	0.46	0.58	0.68	0.47
eeMETRIC	1.71	0.18	84%	0%	0.41	0.95	0.86	0.82
Ensemble	1.11	0.12	55%	0%	0.50	1.00	0.92	0.93
geeSEBAL	0.51	0.18	16%	0%	0.43	0.85	0.88	0.78
PT-JPL	0.87	0.13	43%	0%	0.50	0.96	0.90	0.89
SIMS	2.53	0.12	125%	0%	0.64	1.01	0.91	0.92
SSEBop	1.00	0.13	49%	0%	0.52	0.97	0.90	0.88

492

493 **4. Discussion**

494 We found that there was generally a positive correlation between calculated and reported
495 irrigation at the field, WRG, and management area scales. The agreement was the best at the
496 field scale, where we found that the growing season timescale of aggregation and the OpenET
497 ensemble mean provided the closest match to reported irrigation. At the WRG and management
498 area scales, we observed substantially more variability in the ET-based irrigation calculations
499 than reported irrigation, which appeared to be associated with uncertainties in linking irrigated
500 areas to places of use and non-evaporative components of the water balance, such as deep
501 percolation and runoff used to calculate effective precipitation and year-to-year variability in soil
502 moisture storage. Here, we discuss key sources of uncertainty that may have contributed to
503 differences between reported and calculated irrigation and how those may affect the utility of
504 ET-based irrigation products for research and management.

505

506 *4.1 Sources of uncertainty in estimating irrigation from ET data*

507 We identified and evaluated several sources of uncertainty that may explain differences
508 between satellite ET-based and reported irrigation water withdrawals and applications, including
509 (i) accounting for non-evaporative water balance components such as changes in soil moisture
510 storage and effective precipitation; (ii) accurate identification of irrigated area, including linking
511 fields to wells; and (iii) variability among ET models.

512

513 4.1.1 Soil moisture changes and effective precipitation

514 Quantifying non-evaporative components of the water balance such as year-to-year
515 changes in soil moisture, deep percolation, and runoff appeared to be an important driver of
516 uncertainty in our analysis at all three spatial scales. Since our approach relies on a relatively
517 simple water balance (ET - effective precipitation) to estimate applied irrigation, the positive bias
518 we observe at the WRG and management area scales suggests that we may be underestimating
519 effective precipitation. Therefore, one contributing factor to our observed overestimates of
520 irrigation may be the relatively simple approach we used to estimate effective precipitation,
521 which was based on a regional regression for deep percolation (Figure S3). While runoff may be
522 a source of error in our simple water balance approach for some locations (e.g. fields with larger
523 slopes), it is regionally a small component of the water balance and is unlikely to explain
524 systematic patterns of model errors observed across our study area (Deines et al., 2021). The
525 consistent positive precipitation deficit for rainfed corn (Figure 9) further suggests that effective
526 precipitation is being underestimated by our approach, and calculating effective precipitation
527 using a field-specific soil water balance model approach such as ETDemands (Allen et al., 2020)
528 could help to improve overall agreement. Issues with ET data may also be greater during wet
529 conditions, as we would expect greater errors in calculated ET, and therefore irrigation, for
530 periods or regions with increased cloud cover that affect the optical and thermal bands of
531 satellites used by ET models. Since cloud cover is associated with precipitation events, this may

532 have an outsized effect on estimating ET and irrigation during times when soil moisture is being
533 replenished.

534 While the overall positive bias suggests issues with effective precipitation calculations,
535 the strong relationship between the calculated irrigation residual and precipitation (Figure 8b)
536 suggests that year-to-year changes in root zone soil moisture are also a source of uncertainty.
537 Holding all other aspects of the water balance constant, if soil moisture storage decreased during
538 the dry 2020 growing season, this would cause an increased overestimate of irrigation since
539 some of the ET in 2020 was using soil moisture that fell in previous years, such as the relatively
540 wet 2019. However, variability in individual producer irrigation behavior across years may also
541 contribute to the increased interannual variability in the ET-based irrigation volumes observed in
542 Figure 8 compared to the reported irrigation volumes. For example, previous research in the
543 neighboring state of Nebraska has shown that metered groundwater use typically exceeds crop
544 water requirements in wetter and average rainfall years while farmers are observed to adopt more
545 water-efficient irrigation practices in drier years to reduce non-consumptive water losses, likely
546 motivated by a combination of the higher costs of irrigation and greater likelihood of
547 experiencing irrigation system capacity constraints in drought years (Foster et al., 2019).

548 Furthermore, our ET-based irrigation volumes did not account for leakage in irrigation
549 systems and other losses of water between where it is pumped from the ground but before it
550 reaches the field, though based on the high efficiency in the SD-6 LEMA area we expect that
551 these losses are minimal (~10%, consistent with other estimates). However, in settings with
552 lower irrigation efficiencies, non-consumptive losses of applied irrigation water such as deep
553 percolation or runoff would likely be missed by ET-based irrigation estimation methods and can
554 have a significant impact on estimated irrigation water use (Puy et al., 2022). Our analysis
555 suggests that, for annual or finer temporal resolutions and/or settings with lower irrigation
556 efficiency, the use of more complex water balance approaches, such as soil water balance models
557 (Dhungel et al., 2020; Kharrou et al., 2021; Pereira, Paredes, & Jovanovic, 2020; Zhang et al.,
558 2023), will be necessary to accurately disentangle the rates, locations, and timing of irrigation
559 applications. To facilitate these approaches, there may be promise through the assimilation of
560 additional data sets such as in situ or remotely sensed soil moisture (Dari et al., 2020; Filippelli
561 et al., 2022; Jalilvand et al., 2019, 2023; Laluet et al., 2024; Paolini et al., 2023).

562

563 4.1.2 Linking wells to irrigated fields

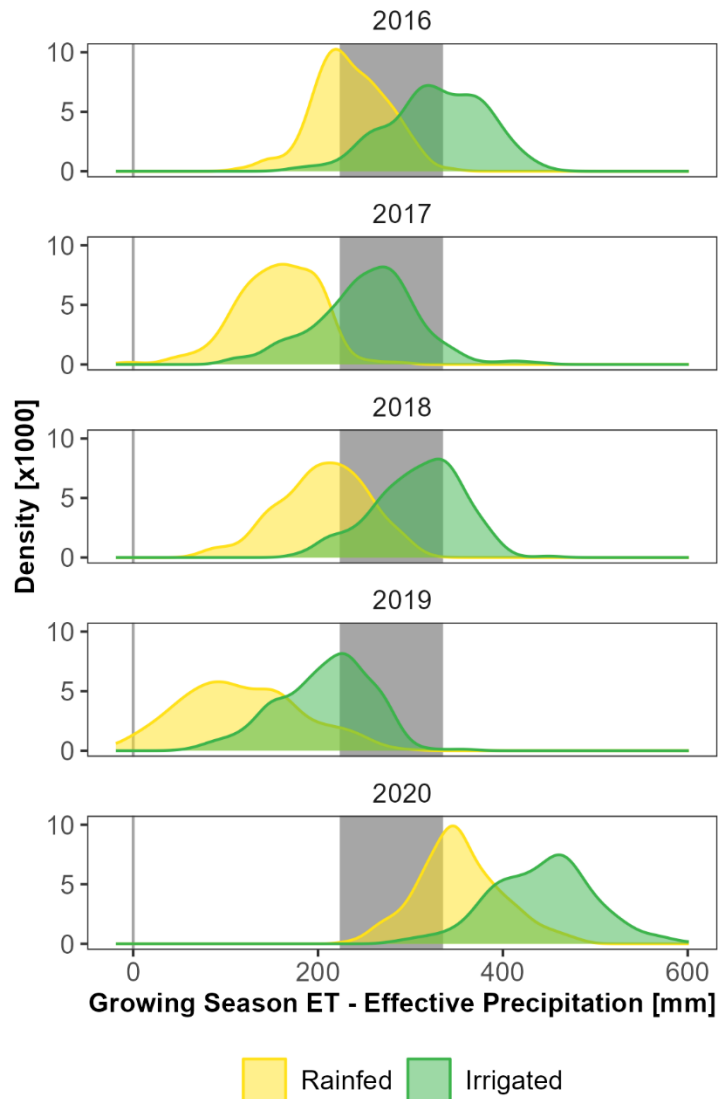
564 Challenges in linking specific wells to irrigated fields appeared to cause disagreement
565 between reported and calculated irrigation at the WRG spatial scale. This source of uncertainty is
566 supported by several lines of evidence. At the field scale, where irrigated extents were known
567 and verified by the farmers sharing their irrigation data, we generally saw the best agreement
568 between calculated and reported irrigation (Figure 4), while at the WRG scale there was
569 substantial disagreement between estimated and reported irrigated area (Figure 6). At the WRG
570 scale, our ET-based calculations of irrigation volume were better correlated with flowmeter data
571 than calculations of irrigation depth (Figure 5), consistent with results from the nearby Colorado

572 portion of the Republican River Basin (Filippelli et al., 2022), and agreement improved when
573 focusing only on WRGs where reported and estimated irrigated area were similar (Figure 7). The
574 weaker relationship between calculated and reported irrigation depth, compared to irrigation
575 volume, reflects the importance of irrigated area as a determinant of overall irrigation volumes
576 (Lamb et al., 2021; Puy et al., 2021; Wei et al., 2022).

577 While the irrigation extent dataset we used is the best-available for this region and
578 consistently shows differences in precipitation deficit between irrigated and rainfed corn, there is
579 also substantial overlap between their distributions, suggesting that some degree of
580 misclassification is practically assured (Figure 9). Based on our analysis, local errors in irrigation
581 status maps are likely fairly evenly distributed between under- and over-estimating irrigated area,
582 with a slight bias towards overestimated irrigated area (Figure 6). This may be particularly
583 challenging in relatively small unirrigated portions of otherwise irrigated fields, such as the non-
584 irrigated corners of center-pivot systems (Figure S5). Additionally, irrigation mapping can be
585 particularly challenging during wet years, such as 2019 when there is the greatest overlap
586 between rainfed and irrigated distributions, because the differences in canopy cover and
587 greenness between irrigated and rainfed fields are smaller (Xu et al., 2019).

588 Accurately linking the point of water diversion with the place where that water is applied
589 was a major challenge in our analysis and has been identified as a key source of uncertainty in
590 other domains (Ott et al., 2024). While developing these links may not be needed for many
591 applications, such as regional water balance assessments, connecting the point of diversion with
592 place of use is critical to evaluate irrigation application depths and to assess the effectiveness of
593 conservation measures and the ultimate impacts of pumping on other aspects of regional
594 agrohydrological systems such as streamflow (Kniffin et al., 2020; Zipper, Carah, et al., 2019;
595 Zipper et al., 2021), aquifer dynamics (Feinstein et al., 2016; Peterson & Fulton, 2019; Wilson et
596 al., 2021), or groundwater-dependent ecosystems (Tolley et al., 2019). Despite exceptionally
597 high-quality water use data for the state of Kansas, the limited linkages between the point of
598 diversion and actual place of use highlights a key data gap for the application of remotely sensed
599 irrigation data for hydrogeological research and management, and a necessary improvement for
600 field-level operationalization.

601



602
603
604
605
606

Figure 9. Distribution of field-resolution growing season ensemble ET - Effective Precipitation for corn fields in the SD-6 LEMA, separated by year and colored by irrigation status. The gray shaded interval shows the average annual LEMA irrigation allocation (279.4 mm) +/- 20%.

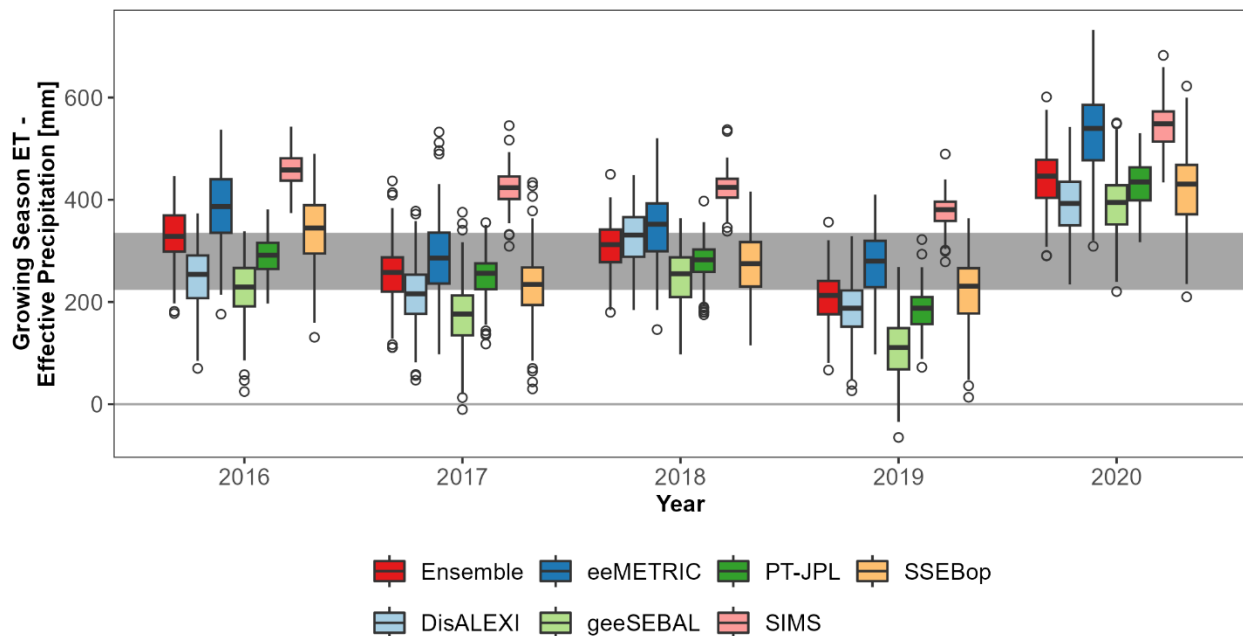
607 4.1.3 Variability among ET models

608 The selection of ET model also led to substantial variability in the estimated irrigation
609 depths, with a relatively consistent ordering across models (from lowest to highest): geeSEBAL,
610 DisALEXI, PT-JPL, SSEBop, Ensemble, eeMETRIC, SIMS (Figure 4, Figure 8). Since the
611 effective precipitation input data used to estimate irrigation was the same for all models, this
612 variability in estimated irrigation among the models can be attributed entirely to differences in
613 the approaches used by each ET model, and variability can be quite substantial. For example, for
614 irrigated corn in the SD-6 LEMA, the medians span 156-270 mm across ET models in a given
615 year (Figure 10), which approaches the magnitude of total applied irrigation water and greatly
616 exceeds the magnitude of the conservation actions put in place in this region (Whittemore et al.,

617 2023). The variability among models may be due to differences in the approaches to computation
 618 of the sensible heat flux used in each of the five energy balance models, differences in the spatial
 619 scale of key meteorological inputs for the DisALEXI, PT-JPL and geeSEBAL models, and
 620 model assumptions, especially for SIMS, which assumes well-watered conditions. This
 621 underscores the importance of local model accuracy assessments to identify the models that
 622 perform best for the crop types and irrigation management practices that are most prevalent in
 623 the region.

624 In the absence of suitable independent dataset for use in a local or regional accuracy
 625 assessment, OpenET recommends use of the ensemble ET value, which has been shown to
 626 perform best overall for the western U.S. across most accuracy metrics (Melton et al., 2022;
 627 Volk et al., 2024). Our results support this recommendation, as we found that the model
 628 ensemble was generally among the best-performing approaches to calculating irrigation (Table 1,
 629 Table 3), particularly after statistically adjusting to account for potential errors in effective
 630 precipitation calculations (Figure 8c). This suggests that the ensemble mean would be a
 631 reasonable approach to use across our study region until additional local accuracy assessments
 632 can be conducted.

633



634
 635 **Figure 10.** Distribution of ET - precipitation for all irrigated corn fields in the LEMA, colored by model.
 636 The gray shaded interval shows the average annual LEMA irrigation allocation (279.4 mm) +/- 20%.

637
 638 *4.2 Utility for research and management purposes*

639 As water becomes increasingly scarce, the importance of accurate accounting of how,
 640 where, when, and how much water is being used is becoming more critical. In the US, each state
 641 is responsible for administering water rights and regulating water use within their jurisdictional
 642 boundaries. Water use metering and reporting requirements vary significantly between states.

643 Satellite-based ET data could provide a nationally consistent approach to computing
644 consumptive use of water applied for irrigation, and potentially for estimating the volume of
645 water applied for crop irrigation, which is the largest source of consumptive water use in the US
646 (Marston et al., 2018). However, these satellite-based irrigation calculations need to be
647 comparable to what is actually happening on the ground, demonstrating the importance of high-
648 fidelity in situ measurements of irrigation. This study was made possible by metered
649 groundwater pumping records detailing the location, amount, and timing of irrigation. Outside of
650 Kansas, metered records of irrigation are rare, with many states not requiring flowmeters on
651 agricultural water uses (Marston, Abdallah, et al., 2022). This gap is increasingly being filled
652 with reanalysis and ET-based water use products (Haynes et al., 2023; Martin et al., 2023). For
653 ET-based irrigation data to become more useful to researchers, irrigators, regulators, and
654 policymakers, metered irrigation records are needed for other areas with different soils, climate,
655 irrigation practices, and cropping patterns to evaluate the performance of ET-based irrigation
656 calculations under these different conditions.

657 The sources of uncertainty we discuss in Section 4.1 contributed to variable levels of
658 agreement between ET-based and reported water withdrawals and applications across the
659 comparisons we conducted. At the field scale, we found a generally low bias and slope
660 approaching one for the ensemble mean irrigation (Table 1), though the R^2 and MAE we
661 observed was lower than assessments elsewhere (e.g., Ott et al., 2024). At the management area,
662 we found a strong positive correlation (e.g., R^2 generally above 0.85; Table 3), comparable to
663 other studies using remotely sensed data to estimate irrigation depths with statistical models
664 (Filippelli et al., 2022; Majumdar et al., 2022; Wei et al., 2022). However, we observed a general
665 positive bias and more year-to-year variability in ET-based irrigation than in the reported data,
666 with substantial improvements in agreement after adjusting for potential effective precipitation
667 (Figure 8c). Agreement between calculated and reported irrigation was the worst for the WRG-
668 scale comparison, in particular for irrigation depths, highlighting the major challenges in linking
669 points of diversion to irrigated field extents.

670 Since errors in estimated irrigation can lead to significant economic and hydrological
671 impacts if used for management purposes (Foster et al., 2020), continued methodological
672 development to overcome the uncertainties described above will be important to advance these
673 tools for some applications. For instance, for purposes that require estimating long-term average
674 consumptive use, such as calculating the water balance for a large (10s to 100s of km) region, the
675 precipitation-adjusted spatially- and temporally-aggregated results we show in Figure 8c might
676 be sufficient. For example, the precipitation-adjusted irrigation calculation approach we show
677 could be effective for providing accurate irrigation calculations extrapolated through space or
678 time. Potential applications may include extending irrigation records backwards to years prior to
679 the onset of irrigation monitoring, providing rapid information on annual irrigation volumes prior
680 to reporting volumes becoming available (a process which typically takes several months in this
681 region), or estimating irrigation in neighboring areas where agricultural practices are similar, but
682 monitoring is unavailable. In areas without any metered data that would be capable for training

683 models, approaches based solely on irrigated area may provide sufficiently accurate water use
684 estimates (Puy et al., 2021), assuming irrigated area is mapped with sufficient accuracy.

685 In contrast, using these data for other purposes, such as monitoring within-season
686 irrigation timing and volume from a specific well, would require significant improvements in the
687 accuracy of calculated irrigation at these finer spatial and temporal scales and careful selection of
688 an appropriate ET model. We found that statistical adjustments to ET-based irrigation
689 calculations can substantially improve agreement with reported values at annual resolution
690 (Figure 8c), potentially suggesting a path towards greater local accuracy, and highlighting the
691 critical importance of accurate effective precipitation values and ground-based data for
692 comparison. While our precipitation-adjusted approach required reported irrigation data, and
693 therefore would not be tractable in locations without existing withdrawal monitoring, it may be
694 possible to use a limited subset of reporting locations to develop relationships that can be applied
695 more broadly (Bohling et al., 2021). Additional products, such as high-resolution soil moisture
696 data from remote sensing-model integration (Vergopolan et al., 2021), may also provide a
697 pathway for bias-correction and/or temporal disaggregation when integrated with field-specific
698 water balance modeling tools (Hoekstra, 2019). Given that OpenET is a relatively new product
699 (Melton et al., 2022), continued work on specific research and management applications will
700 provide useful targets for prioritizing efforts to reduce existing uncertainties.

701

702 **5. Conclusions**

703 We evaluated ET-based calculations of irrigation using a simple water balance approach and
704 compared to reported irrigation from farmer records and a statewide database. We found that the
705 agreement between calculated and reported irrigation was best at the field scale, where irrigated
706 extent was precisely known, and when aggregating ET calculations using the OpenET ensemble
707 mean at the growing season timescale. At the WRG and management area scales, there were
708 generally positive correlations between the ET-based approaches and reported data, but the ET-
709 based approaches typically demonstrated more variability than reported values and overestimated
710 irrigation, particularly during dry years. This may be partially attributed to changes in soil
711 moisture storage, the approach used to calculate effective precipitation, and challenges linking
712 irrigated area to specific fields. The choice of an ET model is an additional source of uncertainty.
713 The uncertainties in ET-based irrigation calculations likely exceed the signal of management
714 activities in this region, suggesting further methodological refinement is needed for applications
715 requiring precise quantification of irrigation depth for a given location and/or single year.
716 However, for applications focused on relative differences in irrigation intensity across space
717 and/or multi-year average irrigation applications, some of these uncertainties may safely be
718 ignored. This work suggests that ET-based approaches to calculating irrigation are a potentially
719 valuable tool for developing improved spatial and temporal water use data and will likely require
720 application-specific targeted improvements to reduce key uncertainties.

721

722 6. Acknowledgments

723 We appreciate assistance from Will Carrara and John Woods with data acquisition/processing
724 and feedback on the manuscript from Sayantan Majumdar (Desert Research Institute). Ashley
725 Grinstead's participation was supported by the Kansas Geological Survey Geohydrology
726 Internship Program (<https://www.kgs.ku.edu/Hydro/gipIndex.html>). We greatly appreciate the
727 farmers who were willing to share their water use data with us. This work was supported by
728 National Aeronautics and Space Administration (NASA) [grant number 80NSSC22K1276] and
729 National Science Foundation (NSF) [grant number RISE-2108196]. TF was also supported by
730 Innovate UK [award number 10044695], as part of the UK Research and Innovation and
731 European Commission funded project 'TRANSCEND: Transformational and robust adaptation
732 to water scarcity and climate change under deep uncertainty'. Data and code used in the study
733 are available at https://github.com/samzipper/SD-6_MapWaterConservation during the review
734 process and will be posted to a repository with a DOI at the time of manuscript acceptance.

735

736 7. References

- 737 Abatzoglou, J. T. (2013). Development of gridded surface meteorological data for ecological
738 applications and modelling. *International Journal of Climatology*, 33(1), 121–131.
739 <https://doi.org/10.1002/joc.3413>
- 740 Allen, R. G., Tasumi, M., Morse, A., & Trezza, R. (2005). A Landsat-based energy balance and
741 evapotranspiration model in Western US water rights regulation and planning. *Irrigation
742 and Drainage Systems*, 19(3), 251–268. <https://doi.org/10.1007/s10795-005-5187-z>
- 743 Allen, R. G., Tasumi, M., Morse, A., Trezza, R., Wright, J. L., Bastiaanssen, W., et al. (2007).
744 Satellite-based energy balance for mapping evapotranspiration with internalized
745 calibration (METRIC)—Applications. *Journal of Irrigation and Drainage Engineering*,
746 133(4), 395–406.
- 747 Allen, R. G., Pereira, L. S., Howell, T. A., & Jensen, M. E. (2011). Evapotranspiration
748 information reporting: I. Factors governing measurement accuracy. *Agricultural Water
749 Management*, 98(6), 899–920. <https://doi.org/10.1016/j.agwat.2010.12.015>
- 750 Allen, R. G., Robison, C. W., Huntington, J., Wright, J. L., & Kilic, A. (2020). Applying the
751 FAO-56 dual Kc method for irrigation water requirements over large areas of the
752 Western US. *Transactions of the ASABE*, 63(6), 2059–2081.
753 <https://doi.org/10.13031/trans.13933>
- 754 Anderson, M. C., Norman, J. M., Mecikalski, J. R., Otkin, J. A., & Kustas, W. P. (2007). A
755 climatological study of evapotranspiration and moisture stress across the continental
756 United States based on thermal remote sensing: 1. Model formulation. *Journal of
757 Geophysical Research: Atmospheres*, 112(D10). <https://doi.org/10.1029/2006JD007506>
- 758 Anderson, M. C., Gao, F., Knipper, K., Hain, C., Dulaney, W., Baldocchi, D., et al. (2018).
759 Field-Scale Assessment of Land and Water Use Change over the California Delta Using
760 Remote Sensing. *Remote Sensing*, 10(6), 889. <https://doi.org/10.3390/rs10060889>
- 761 Bastiaanssen, W. G. M., Menenti, M., Feddes, R. A., & Holtslag, A. A. M. (1998). A remote
762 sensing surface energy balance algorithm for land (SEBAL). 1. Formulation. *Journal of
763 Hydrology*, 212, 198–212.
- 764 Bohling, G. C., Butler, J. J., Whittemore, D. O., & Wilson, B. B. (2021). Evaluation of Data
765 Needs for Assessments of Aquifers Supporting Irrigated Agriculture. *Water Resources*

766 *Research*, 57(4), e2020WR028320. <https://doi.org/10.1029/2020WR028320>

767 Brocca, L., Tarpanelli, A., Filippucci, P., Dorigo, W., Zaussinger, F., Gruber, A., & Fernández-
768 Prieto, D. (2018). How much water is used for irrigation? A new approach exploiting
769 coarse resolution satellite soil moisture products. *International Journal of Applied Earth*
770 *Observation and Geoinformation*, 73, 752–766. <https://doi.org/10.1016/j.jag.2018.08.023>

771 Brookfield, A. E., Zipper, S., Kendall, A. D., Ajami, H., & Deines, J. M. (2024). Estimating
772 Groundwater Pumping for Irrigation: A Method Comparison. *Groundwater*, 62(1), 15–
773 33. <https://doi.org/10.1111/gwat.13336>

774 Butler, J. J., Whittemore, D. O., Wilson, B. B., & Bohling, G. C. (2016). A new approach for
775 assessing the future of aquifers supporting irrigated agriculture. *Geophysical Research*
776 *Letters*, 43(5), 2004–2010. <https://doi.org/10.1002/2016GL067879>

777 Butler, J. J., Bohling, G. C., Whittemore, D. O., & Wilson, B. B. (2020). Charting Pathways
778 Toward Sustainability for Aquifers Supporting Irrigated Agriculture. *Water Resources*
779 *Research*, 56(10), e2020WR027961. <https://doi.org/10.1029/2020WR027961>

780 Dalin, C., Wada, Y., Kastner, T., & Puma, M. J. (2017). Groundwater depletion embedded in
781 international food trade. *Nature*, 543(7647), 700–704.
782 <https://doi.org/10.1038/nature21403>

783 Dari, J., Brocca, L., Quintana-Seguí, P., Escorihuela, M. J., Stefan, V., & Morbidelli, R. (2020).
784 Exploiting High-Resolution Remote Sensing Soil Moisture to Estimate Irrigation Water
785 Amounts over a Mediterranean Region. *Remote Sensing*, 12(16), 2593.
786 <https://doi.org/10.3390/rs12162593>

787 Deines, J. M., Kendall, A. D., Crowley, M. A., Rapp, J., Cardille, J. A., & Hyndman, D. W.
788 (2019). Mapping three decades of annual irrigation across the US High Plains Aquifer
789 using Landsat and Google Earth Engine. *Remote Sensing of Environment*, 233, 111400.
790 <https://doi.org/10.1016/j.rse.2019.111400>

791 Deines, J. M., Kendall, A. D., Butler, J. J., & Hyndman, D. W. (2019). Quantifying irrigation
792 adaptation strategies in response to stakeholder-driven groundwater management in the
793 US High Plains Aquifer. *Environmental Research Letters*, 14(4), 044014.
794 <https://doi.org/10.1088/1748-9326/aafe39>

795 Deines, J. M., Schipanski, M. E., Golden, B., Zipper, S. C., Nozari, S., Rottler, C., et al. (2020).
796 Transitions from irrigated to dryland agriculture in the Ogallala Aquifer: Land use
797 suitability and regional economic impacts. *Agricultural Water Management*, 233,
798 106061. <https://doi.org/10.1016/j.agwat.2020.106061>

799 Deines, J. M., Kendall, A. D., Butler, J. J., Basso, B., & Hyndman, D. W. (2021). Combining
800 Remote Sensing and Crop Models to Assess the Sustainability of Stakeholder-Driven
801 Groundwater Management in the US High Plains Aquifer. *Water Resources Research*,
802 e2020WR027756. <https://doi.org/10.1029/2020WR027756>

803 Dhungel, R., Aiken, R., Lin, X., Kenyon, S., Colaizzi, P. D., Luhman, R., et al. (2020).
804 Restricted water allocations: Landscape-scale energy balance simulations and
805 adjustments in agricultural water applications. *Agricultural Water Management*, 227,
806 105854. <https://doi.org/10.1016/j.agwat.2019.105854>

807 D’Odorico, P., Carr, J., Dalin, C., Dell’Angelo, J., Konar, M., Laio, F., et al. (2019). Global
808 virtual water trade and the hydrological cycle: patterns, drivers, and socio-environmental
809 impacts. *Environmental Research Letters*, 14(5), 053001. <https://doi.org/10.1088/1748-9326/ab05f4>

810

811 Drysdale, K. M., & Hendricks, N. P. (2018). Adaptation to an irrigation water restriction

812 imposed through local governance. *Journal of Environmental Economics and*
813 *Management*, 91, 150–165. <https://doi.org/10.1016/j.jeem.2018.08.002>

814 Earnhart, D., & Hendricks, N. P. (2023). Adapting to water restrictions: Intensive versus
815 extensive adaptation over time differentiated by water right seniority. *American Journal*
816 *of Agricultural Economics*. <https://doi.org/10.1111/ajae.12361>

817 Feinstein, D. T., Fienen, M. N., Reeves, H. W., & Langevin, C. D. (2016). A Semi-Structured
818 MODFLOW-USG Model to Evaluate Local Water Sources to Wells for Decision
819 Support. *Groundwater*, 54(4), 532–544. <https://doi.org/10.1111/gwat.12389>

820 Filippelli, S. K., Sloggy, M. R., Vogeler, J. C., Manning, D. T., Goemans, C., & Senay, G. B.
821 (2022). Remote sensing of field-scale irrigation withdrawals in the central Ogallala
822 aquifer region. *Agricultural Water Management*, 271, 107764.
823 <https://doi.org/10.1016/j.agwat.2022.107764>

824 Fisher, J. B., Tu, K. P., & Baldocchi, D. D. (2008). Global estimates of the land–atmosphere
825 water flux based on monthly AVHRR and ISLSCP-II data, validated at 16 FLUXNET
826 sites. *Remote Sensing of Environment*, 112(3), 901–919.
827 <https://doi.org/10.1016/j.rse.2007.06.025>

828 Folhes, M. T., Rennó, C. D., & Soares, J. V. (2009). Remote sensing for irrigation water
829 management in the semi-arid Northeast of Brazil. *Agricultural Water Management*,
830 96(10), 1398–1408. <https://doi.org/10.1016/j.agwat.2009.04.021>

831 Foster, T., Gonçalves, I. Z., Campos, I., Neale, C. M. U., & Brozović, N. (2019). Assessing
832 landscape scale heterogeneity in irrigation water use with remote sensing and in situ
833 monitoring. *Environmental Research Letters*, 14(2), 024004.
834 <https://doi.org/10.1088/1748-9326/aaf2be>

835 Foster, T., Mieno, T., & Brozović, N. (2020). Satellite-Based Monitoring of Irrigation Water
836 Use: Assessing Measurement Errors and Their Implications for Agricultural Water
837 Management Policy. *Water Resources Research*, 56(11), e2020WR028378.
838 <https://doi.org/10.1029/2020WR028378>

839 Gao, J., Sheshukov, A. Y., Yen, H., Kastens, J. H., & Peterson, D. L. (2017). Impacts of
840 incorporating dominant crop rotation patterns as primary land use change on hydrologic
841 model performance. *Agriculture, Ecosystems & Environment*, 247, 33–42.
842 <https://doi.org/10.1016/j.agee.2017.06.019>

843 Gibson, J., Franz, T. E., Wang, T., Gates, J., Grassini, P., Yang, H., & Eisenhauer, D. (2017). A
844 case study of field-scale maize irrigation patterns in western Nebraska: implications for
845 water managers and recommendations for hyper-resolution land surface modeling.
846 *Hydrology and Earth System Sciences*, 21(2), 1051–1062. [https://doi.org/10.5194/hess-](https://doi.org/10.5194/hess-21-1051-2017)
847 [21-1051-2017](https://doi.org/10.5194/hess-21-1051-2017)

848 Gleeson, T., Cuthbert, M., Ferguson, G., & Perrone, D. (2020). Global Groundwater
849 Sustainability, Resources, and Systems in the Anthropocene. *Annual Review of Earth and*
850 *Planetary Sciences*, 48(1). <https://doi.org/10.1146/annurev-earth-071719-055251>

851 Glose, T. J., Zipper, S., Hyndman, D. W., Kendall, A. D., Deines, J. M., & Butler, J. J. (2022).
852 Quantifying the impact of lagged hydrological responses on the effectiveness of
853 groundwater conservation. *Water Resources Research*, 58(7), e2022WR032295.
854 <https://doi.org/10.1029/2022WR032295>

855 Golden, B. (2018). *Monitoring the Impacts of Sheridan County 6 Local Enhanced Management*
856 *Area*. Kansas State University. Retrieved from [https://agriculture.ks.gov/docs/default-](https://agriculture.ks.gov/docs/default-source/dwr-water-appropriation-documents/sheridancounty6_lemma_goldenreport_2013-)
857 [source/dwr-water-appropriation-documents/sheridancounty6_lemma_goldenreport_2013-](https://agriculture.ks.gov/docs/default-source/dwr-water-appropriation-documents/sheridancounty6_lemma_goldenreport_2013-)

2017.pdf?sfvrsn=dac48ac1_0

de Graaf, I. E. M., Gleeson, T., Beek, L. P. H. (Rens) van, Sutanudjaja, E. H., & Bierkens, M. F. P. (2019). Environmental flow limits to global groundwater pumping. *Nature*, *574*(7776), 90–94. <https://doi.org/10.1038/s41586-019-1594-4>

Hasan, M. F., Smith, R., Vajedian, S., Pommerenke, R., & Majumdar, S. (2023). Global land subsidence mapping reveals widespread loss of aquifer storage capacity. *Nature Communications*, *14*(1), 6180. <https://doi.org/10.1038/s41467-023-41933-z>

Haynes, J. V., Read, A. L., Chan, A. Y., Martin, D. J., Regan, R. S., Henson, W., et al. (2023). Monthly crop irrigation withdrawals and efficiencies by HUC12 watershed for years 2000-2020 within the conterminous United States [Data set]. U.S. Geological Survey. <https://doi.org/10.5066/P9LGISUM>

Hoekstra, A. Y. (2019). Green-blue water accounting in a soil water balance. *Advances in Water Resources*, *129*, 112–117. <https://doi.org/10.1016/j.advwatres.2019.05.012>

Jalilvand, E., Abolafia-Rosenzweig, R., Tajrishy, M., Kumar, S. V., Mohammadi, M. R., & Das, N. N. (2023). Is It Possible to Quantify Irrigation Water-Use by Assimilating a High-Resolution Satellite Soil Moisture Product? *Water Resources Research*, *59*, e2022WR033342. <https://doi.org/10.1029/2022WR033342>

Jalilvand, E., Tajrishy, M., Ghazi Zadeh Hashemi, S. A., & Brocca, L. (2019). Quantification of irrigation water using remote sensing of soil moisture in a semi-arid region. *Remote Sensing of Environment*, *231*, 111226. <https://doi.org/10.1016/j.rse.2019.111226>

Jasechko, S., Seybold, H., Perrone, D., Fan, Y., Shamsudduha, M., Taylor, R. G., et al. (2024). Rapid groundwater decline and some cases of recovery in aquifers globally. *Nature*, *625*(7996), 715–721. <https://doi.org/10.1038/s41586-023-06879-8>

Ketchum, D., Hoylman, Z. H., Huntington, J., Brinkerhoff, D., & Jencso, K. G. (2023). Irrigation intensification impacts sustainability of streamflow in the Western United States. *Communications Earth & Environment*, *4*(1), 1–8. <https://doi.org/10.1038/s43247-023-01152-2>

Kharrou, M. H., Simonneaux, V., Er-Raki, S., Le Page, M., Khabba, S., & Chehbouni, A. (2021). Assessing Irrigation Water Use with Remote Sensing-Based Soil Water Balance at an Irrigation Scheme Level in a Semi-Arid Region of Morocco. *Remote Sensing*, *13*(6), 1133. <https://doi.org/10.3390/rs13061133>

Kniffin, M., Bradbury, K. R., Fienen, M., & Genskow, K. (2020). Groundwater Model Simulations of Stakeholder-Identified Scenarios in a High-Conflict Irrigated Area. *Groundwater*, *58*(6), 973–986. <https://doi.org/10.1111/gwat.12989>

Laipelt, L., Henrique Bloedow Kayser, R., Santos Fleischmann, A., Ruhoff, A., Bastiaanssen, W., Erickson, T. A., & Melton, F. (2021). Long-term monitoring of evapotranspiration using the SEBAL algorithm and Google Earth Engine cloud computing. *ISPRS Journal of Photogrammetry and Remote Sensing*, *178*, 81–96. <https://doi.org/10.1016/j.isprsjprs.2021.05.018>

Laluet, P., Olivera-Guerra, L. E., Altés, V., Paolini, G., Ouaadi, N., Rivalland, V., Jarlan, L., Villar, J. M., & Merlin, O. (2024). Retrieving the irrigation actually applied at district scale: Assimilating high-resolution Sentinel-1-derived soil moisture data into a FAO-56-based model. *Agricultural Water Management*, *293*, 108704. <https://doi.org/10.1016/j.agwat.2024.108704>

Lamb, S. E., Haacker, E. M. K., & Smidt, S. J. (2021). Influence of Irrigation Drivers Using Boosted Regression Trees: Kansas High Plains. *Water Resources Research*, *57*(5),

904 e2020WR028867. <https://doi.org/10.1029/2020WR028867>

905 Majumdar, S., Smith, R., Conway, B. D., & Lakshmi, V. (2022). Advancing remote sensing and
906 machine learning-driven frameworks for groundwater withdrawal estimation in Arizona:
907 Linking land subsidence to groundwater withdrawals. *Hydrological Processes*, 36(11),
908 e14757. <https://doi.org/10.1002/hyp.14757>

909 MardanDoost, B., Brookfield, A. E., Feddema, J., Sturm, B., Kastens, J., Peterson, D., & Bishop,
910 C. (2019). Estimating irrigation demand with geospatial and in-situ data: Application to
911 the high plains aquifer, Kansas, USA. *Agricultural Water Management*, 223, 105675.
912 <https://doi.org/10.1016/j.agwat.2019.06.010>

913 Marston, L. T., Ao, Y., Konar, M., Mekonnen, M. M., & Hoekstra, A. Y. (2018). High-
914 Resolution Water Footprints of Production of the United States. *Water Resources*
915 *Research*, 54(3), 2288–2316. <https://doi.org/10.1002/2017WR021923>

916 Marston, L. T., Lamsal, G., Ancona, Z. H., Caldwell, P., Richter, B. D., Ruddell, B. L., et al.
917 (2020). Reducing water scarcity by improving water productivity in the United States.
918 *Environmental Research Letters*, 15(9), 094033. [https://doi.org/10.1088/1748-](https://doi.org/10.1088/1748-9326/ab9d39)
919 [9326/ab9d39](https://doi.org/10.1088/1748-9326/ab9d39)

920 Marston, L. T., Zipper, S., Smith, S. M., Allen, J. J., Butler, J. J., Gautam, S., & Yu, D. J. (2022).
921 The importance of fit in groundwater self-governance. *Environmental Research Letters*,
922 17(11), 111001. <https://doi.org/10.1088/1748-9326/ac9a5e>

923 Marston, L. T., Abdallah, A. M., Bagstad, K. J., Dickson, K., Glynn, P., Larsen, S. G., et al.
924 (2022). Water-Use Data in the United States: Challenges and Future Directions. *JAWRA*
925 *Journal of the American Water Resources Association*, 58(4), 485–495.
926 <https://doi.org/10.1111/1752-1688.13004>

927 Martin, D., Regan, R. S., Haynes, J. V., Read, A. L., Henson, W., Stewart, J. S., et al. (2023).
928 Irrigation water use reanalysis for the 2000-20 period by HUC12, month, and year for the
929 conterminous United States [Data set]. U.S. Geological Survey.
930 <https://doi.org/10.5066/P9YWR00J>

931 Melton, F. S., Johnson, L. F., Lund, C. P., Pierce, L. L., Michaelis, A. R., Hiatt, S. H., et al.
932 (2012). Satellite Irrigation Management Support With the Terrestrial Observation and
933 Prediction System: A Framework for Integration of Satellite and Surface Observations to
934 Support Improvements in Agricultural Water Resource Management. *IEEE Journal of*
935 *Selected Topics in Applied Earth Observations and Remote Sensing*, 5(6), 1709–1721.
936 <https://doi.org/10.1109/JSTARS.2012.2214474>

937 Melton, F. S., Huntington, J., Grimm, R., Herring, J., Hall, M., Rollison, D., et al. (2022).
938 OpenET: Filling a Critical Data Gap in Water Management for the Western United
939 States. *JAWRA Journal of the American Water Resources Association*, 58(6), 971–994.
940 <https://doi.org/10.1111/1752-1688.12956>

941 Mourtzinis, S., Rattalino Edreira, J. I., Conley, S. P., & Grassini, P. (2017). From grid to field:
942 Assessing quality of gridded weather data for agricultural applications. *European Journal*
943 *of Agronomy*, 82, 163–172. <https://doi.org/10.1016/j.eja.2016.10.013>

944 Ott, T. J., Majumdar, S., Huntington, J., Pearson, C., Bromley, M., Minor, B. A., et al. (2024).
945 Toward Sustainable Groundwater Management: Harnessing Remote Sensing and Climate
946 Data to Estimate Field-Scale Groundwater Pumping. *ESS Open Archive*.
947 <https://doi.org/10.22541/essoar.170800918.86740881/v1>

948 Paolini, G., Escorihuela, M.J., Merlin, O., Lалуé, P., Bellvert, J., & Pellarin, T. (2023).
949 Estimating multi-scale irrigation amounts using multi-resolution soil moisture data: A

950 data-driven approach using PrISM. *Agricultural Water Management*, 290, 108594.
951 <https://doi.org/10.1016/j.agwat.2023.108594>

952 Pereira, L. S., Paredes, P., Melton, F., Johnson, L., Wang, T., López-Urrea, R., et al. (2020).
953 Prediction of crop coefficients from fraction of ground cover and height. Background and
954 validation using ground and remote sensing data. *Agricultural Water Management*, 241,
955 106197. <https://doi.org/10.1016/j.agwat.2020.106197>

956 Pereira, L. S., Paredes, P., & Jovanovic, N. (2020). Soil water balance models for determining
957 crop water and irrigation requirements and irrigation scheduling focusing on the FAO56
958 method and the dual Kc approach. *Agricultural Water Management*, 241, 106357.
959 <https://doi.org/10.1016/j.agwat.2020.106357>

960 Peterson, T. J., & Fulton, S. (2019). Joint Estimation of Gross Recharge, Groundwater Usage,
961 and Hydraulic Properties within HydroSight. *Groundwater*, 57(6), 860–876.
962 <https://doi.org/10.1111/gwat.12946>

963 Puy, A., Borgonovo, E., Lo Piano, S., Levin, S.A., & Saltelli, A. (2021). Irrigated areas drive
964 irrigation water withdrawals. *Nature Communications*, 12, 4525.
965 <https://doi.org/10.1038/s41467-021-24508-8>

966 Puy, A., Lankford, B., Meier, J., Kooij, S. van der, & Saltelli, A. (2022). Large variations in
967 global irrigation withdrawals caused by uncertain irrigation efficiencies. *Environmental*
968 *Research Letters*, 17, 044014. <https://doi.org/10.1088/1748-9326/ac5768>

969 Senay, G. B., Friedrichs, M., Morton, C., Parrish, G. E. L., Schauer, M., Khand, K., et al. (2022).
970 Mapping actual evapotranspiration using Landsat for the conterminous United States:
971 Google Earth Engine implementation and assessment of the SSEBop model. *Remote*
972 *Sensing of Environment*, 275, 113011. <https://doi.org/10.1016/j.rse.2022.113011>

973 Steiner, J. L., Devlin, D. L., Perkins, S., Aguilar, J. P., Golden, B., Santos, E. A., & Unruh, M.
974 (2021). Policy, Technology, and Management Options for Water Conservation in the
975 Ogallala Aquifer in Kansas, USA. *Water*, 13(23), 3406.
976 <https://doi.org/10.3390/w13233406>

977 Tolley, D., Foglia, L., & Harter, T. (2019). Sensitivity Analysis and Calibration of an Integrated
978 Hydrologic Model in an Irrigated Agricultural Basin With a Groundwater-Dependent
979 Ecosystem. *Water Resources Research*, 55(9), 7876–7901.
980 <https://doi.org/10.1029/2018WR024209>

981 USDA. (2022). *Cropland Data Layer [Online]*. Washington, D.C.: USDA National Agricultural
982 Statistics Service. Retrieved from <https://nassgeodata.gmu.edu/CropScape/>

983 Vergopolan, N., Chaney, N. W., Pan, M., Sheffield, J., Beck, H. E., Ferguson, C. R., et al.
984 (2021). SMAP-HydroBlocks, a 30-m satellite-based soil moisture dataset for the
985 conterminous US. *Scientific Data*, 8(1), 264. <https://doi.org/10.1038/s41597-021-01050-2>

986 Volk, J. M., Huntington, J. L., Melton, F. S., Allen, R., Anderson, M., Fisher, J. B., et al. (2024).
987 Assessing the accuracy of OpenET satellite-based evapotranspiration data to support
988 water resource and land management applications. *Nature Water*, 1–13.
989 <https://doi.org/10.1038/s44221-023-00181-7>

990 Wei, S., Xu, T., Niu, G.-Y., & Zeng, R. (2022). Estimating Irrigation Water Consumption Using
991 Machine Learning and Remote Sensing Data in Kansas High Plains. *Remote Sensing*,
992 14(13), 3004. <https://doi.org/10.3390/rs14133004>

993 Whittemore, D. O., Butler, J. J., Bohling, G. C., & Wilson, B. B. (2023). Are we saving water?
994 Simple methods for assessing the effectiveness of groundwater conservation measures.
995 *Agricultural Water Management*, 287, 108408.

996 <https://doi.org/10.1016/j.agwat.2023.108408>
997 Wilson, B. B., Liu, G., Bohling, G. C., & Butler, J. J. (2021). *GMD4 Groundwater Flow Model:
998 High Plains Aquifer Modeling Maintenance Project* (KGS Open File Report 2021-6).
999 Lawrence KS.

1000 Xu, T., Deines, J. M., Kendall, A. D., Basso, B., & Hyndman, D. W. (2019). Addressing
1001 Challenges for Mapping Irrigated Fields in Subhumid Temperate Regions by Integrating
1002 Remote Sensing and Hydroclimatic Data. *Remote Sensing*, *11*(3), 370.
1003 <https://doi.org/10.3390/rs11030370>

1004 Zhang, J., Guan, K., Zhou, W., Jiang, C., Peng, B., Pan, M., Grant, R.F., Franz, T.E., Suyker, A.,
1005 Yang, Y., Chen, X., Lin, K., & Ma, Z. (2023). Combining Remotely Sensed
1006 Evapotranspiration and an Agroecosystem Model to Estimate Center-Pivot Irrigation
1007 Water Use at High Spatio-Temporal Resolution. *Water Resources Research*, *59*,
1008 e2022WR032967. <https://doi.org/10.1029/2022WR032967>

1009 Zipper, S. C., Stack Whitney, K., Deines, J. M., Befus, K. M., Bhatia, U., Albers, S. J., et al.
1010 (2019). Balancing Open Science and Data Privacy in the Water Sciences. *Water
1011 Resources Research*, *55*(7), 5202–5211. <https://doi.org/10.1029/2019WR025080>

1012 Zipper, S. C., Carah, J. K., Dillis, C., Gleeson, T., Kerr, B., Rohde, M. M., et al. (2019).
1013 Cannabis and residential groundwater pumping impacts on streamflow and ecosystems in
1014 Northern California. *Environmental Research Communications*, *1*(12), 125005.
1015 <https://doi.org/10.1088/2515-7620/ab534d>

1016 Zipper, S. C., Gleeson, T., Li, Q., & Kerr, B. (2021). Comparing Streamflow Depletion
1017 Estimation Approaches in a Heavily Stressed, Conjunctively Managed Aquifer. *Water
1018 Resources Research*, *57*(2), e2020WR027591. <https://doi.org/10.1029/2020WR027591>

1019 Zipper, S. C., Farmer, W. H., Brookfield, A., Ajami, H., Reeves, H. W., Wardropper, C., et al.
1020 (2022). Quantifying Streamflow Depletion from Groundwater Pumping: A Practical
1021 Review of Past and Emerging Approaches for Water Management. *JAWRA Journal of
1022 the American Water Resources Association*, *58*(2), 289–312.
1023 <https://doi.org/10.1111/1752-1688.12998>
1024